Available online at www.sciencedirect.com
ScienceDirect
Chemical Geology 247 (2008) 208–228
CHEMICAL GEOLOGY INCLUDING ISOTOPE GEOSCIENCE
www.elsevier.com/locate/chemgeo

Source, transport, and fate of rhenium, selenium, molybdenum, arsenic, and copper in groundwater associated with porphyry–Cu deposits, Atacama Desert, Chile

Matthew I. Leybourne [a,*], Eion M. Cameron [b]

[a] GNS Science, P.O. Box 30-368, Lower Hutt, New Zealand
[b] Eion Cameron Geochemical Inc., 865 Spruce Ridge Road, Carp, Ontario, Canada K0A 1L0

Received 7 December 2006; received in revised form 15 October 2007; accepted 21 October 2007

Editor: D. Rickard

Abstract

We collected groundwaters in and around a large (313 Mt at 1.08% Cu and 0.3% cutoff) undisturbed porphyry copper deposit (Spence) in the hyperarid Atacama Desert of northern Chile, which is buried beneath 30–180 m of Miocene piedmont gravels. Groundwaters within and down-flow of the Spence deposit have elevated Se (up to 800 μg/l), Re (up to 31 μg/l), Mo (up to 475 μg/l) and As (up to 278 μg/l) concentrations compared to up-flow waters (interpreted to represent regional groundwater flow). In contrast, Cu is only elevated (up to 2036 μg/l) in groundwaters recovered from within the deposit; Cu concentrations are low down gradient of the deposit. The differential behavior of the metals/metalloids occurs because the former group dissolves as anions, enhancing their mobility, whereas the base metals dissolve as cations and are lost from solution most likely through adsorption to clay surface exchange sites and through formation of secondary copper chlorides, carbonates, and oxides. Most groundwaters within and down-flow of the deposit have Eh–pH values around the Fe^{II}/Fe^{III} phase boundary, limiting the impact of Fe-oxyhydroxides on oxyanions mobility. Se, Re, Mo, and As are all mobile (with filtered/unfiltered samples ~1) to the limit of sampling 2 km down gradient from the deposit. The increase in ore-related metals, metalloids, and sulfate and decrease in sulfate–S isotope ratios (from values similar to regional salars, +4 to +8‰ $\delta^{34}S_{CDT}$ to lower values closer to hypogene sulfides, +1 to +4‰ $\delta^{34}S_{CDT}$) is consistent with active water–rock reactions between saline groundwaters and the Spence deposit. It is likely that hypogene and/or supergene sulfides are being oxidized under the present groundwater conditions and mineral saturation calculations suggest that secondary copper minerals (antlerite, atacamite, malachite) may also be actively forming, suggesting that supergene and exotic copper mineralization is possible even under the present hyperarid climate of the Atacama Desert.

Keywords: Groundwater; Porphyry copper; Selenium; Rhenium; Arsenic; Molybdenum

1. Introduction

Elevated trace metal and metalloid concentrations in aqueous systems are increasingly recognized as an important health hazard (Selinus et al., 2005). One of the

* Corresponding author. Tel.: +1 64 4 570 4693; fax: +1 64 4 570 4600.
E-mail address: m.leybourne@gns.cri.nz (M.I. Leybourne).

0009-2541/$ - see front matter © 2007 Elsevier B.V. All rights reserved.
doi:10.1016/j.chemgeo.2007.10.017

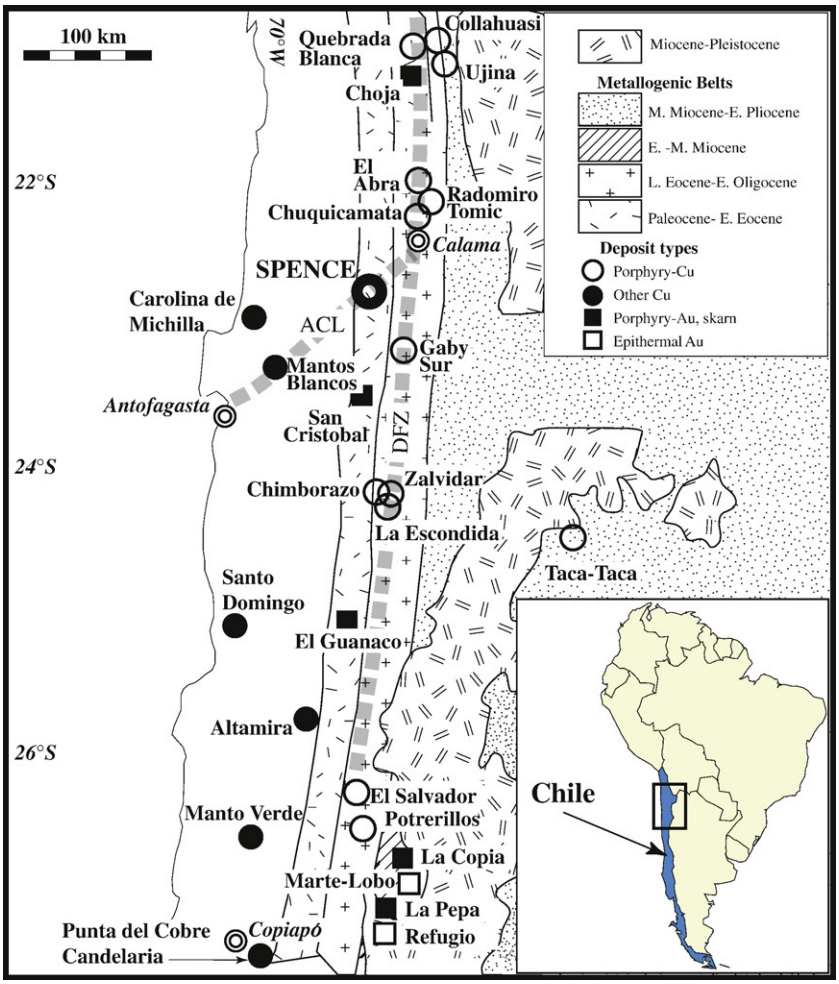

Fig. 1. Regional geology of northern Chile, showing major ore deposits in relation to the geologic belts that host them (modified from Sillitoe, 1992; Richards et al., 1999). The north–south dashed line is the Domeyko Fault Zone (DFZ) and the northeast-southwest dashed line is the Antofagasta–Calama lineament (ACL), as discussed in the text (after Palacios et al., 2007).

difficulties in environmental research is establishing the relative contributions of metals and metalloids from geogenic (natural) and anthropogenic sources (Rasmussen et al., 1998). Undisturbed ore deposits provide natural laboratories of point source "contamination", with groundwater–deposit interactions resulting in metal abundances at levels commonly well in excess of background or health guidelines. For example, volcanic terrain and geothermal waters in northern Chile have elevated As concentrations, which contaminate regional water supplies (Romero et al., 2003). There is a need then to better understand the sources, mobility, pathways, redox speciation and attenuation of trace metals and metalloids in aqueous systems, in particular because the solubility, bioavailability and toxicity of polyvalent metals and metalloids is controlled by redox chemistry (Myneni et al., 1997). Several species of interest in porphyry copper systems are also important as they are direct byproducts of radioactive waste e.g., ^{79}Se with half-life of 6.5×10^4 years (Tachi et al., 1998), or are analogs for nuclear waste products e.g., Re behaves similarly to ^{99}Tc (Xiong and Wood, 1999). Improved understanding of metalloid speciation and mobility will also be of use in management of Se contamination through anthropogenic activity (Peters et al., 1999), As contamination through changes in groundwater management practices (Horneman et al., 2004; Van Geen et al., 2004; Thoral et al., 2005), and naturally anomalous areas such as the Atacama Desert. Finally, the speciation and transport mechanisms of Se and associated metalloids are also of interest because of applications with respect to mineral exploration and

environmental base-line studies (Cameron et al., 2004; Leybourne, 2007).

In this paper, we report on elevated Cu, Se, As, Mo and Re concentrations in groundwaters recovered in and around the large Spence porphyry copper deposit in the hyperarid Atacama Desert of northern Chile. The purposes of this study are to determine: 1) the sources of elevated metals and metalloids in groundwaters interacting with porphyry copper mineralization in northern Chile; 2) the style of water–deposit interaction occurring; 3) the extent of transport of porphyry-associated metals and metalloids; and 4) mechanisms of metal and metalloid attenuation. We show in this paper that the concentration of porphyry copper deposit-associated metals and metalloids in groundwaters in this hyperarid climate is a consequence of water–rock interaction and further demonstrate that these species are stable in solution for relatively long transport distances (>1 km), compared to metals that complex as cations, such as Cu (≪1 km).

2. Geological setting

Chile is host to a large number of copper deposits (such as Chuquicamata, Escondida, El Salvador, Collahuasi and Spence) related to major porphyry intrusions that occur within a narrow belt in northern Chile (Fig. 1). These porphyry copper deposits were produced by hydrothermal systems associated with Cenozoic continental arc magmatism (e.g., Sillitoe, 2000; Tosdal and Richards, 2001). Porphyry intrusions were focused along major, long-lived fault systems, with many of the largest deposits associated with the West Fault or Domeyko Fault Zone (DFZ; Fig. 1). The Spence deposit coincides with a major north-northeast lineament that extends from the coast through the town of Calama (Antofagasta–Calama Lineament; ACL) and intersects the DFZ (Fig. 1).

Porphyry copper deposits in northern Chile may contain supergene-enriched high-grade ores (Chávez, 2000; Cuadra and Rojas, 2001). Supergene alteration occurred in the mid-Miocene as the climate of northern Chile became progressively more arid, which, in conjunction with regional uplift, resulted in falling water tables; hypogene sulfide minerals were oxidized with subsequent downward migration of Cu and other associated species. Below the water table, increasingly reducing conditions caused the removal of Cu from solution, either as secondary oxides, carbonates, sulfates or clays (oxide zone), or as secondary chalcocite and/or covellite replacing of primary bornite and chalcopyrite (supergene zone) (Chávez, 2000). Following supergene enrichment, thick piedmont gravels were deposited, as the climate of northern Chile became hyperarid beginning around 14 Ma (Alpers and Brimhall, 1988), although more recent age dating of K-bearing supergene minerals and sedimentological evidence suggests that supergene oxidation may have continued until 3–6 Ma (Hartley and Rice, 2005). In addition, the presence of atacamite ($Cu_2(OH)_3Cl$) and/or paratacamite (atacamite polymorph) in Miocene gravels overlying some supergene zones suggests that some secondary mineralization may be relatively recent (Cameron et al., 2007).

The Spence deposit was discovered in 1996–1997 by RioChilex (now part of BHP-Billiton Ltd.) via grid drilling through the Miocene piedmont gravels that blanket the deposit. The Spence deposit is a large (313.1 Mt at >1.08% Cu, at a Cu cutoff of 0.3% total Cu; (BHP-Billiton, 2007) porphyry deposit, with mineralization having occurred at around 57 Ma (Rowland and Clark, 2001). Three quartz–feldspar porphyries intrude andesitic volcanic rocks (Fig. 2A) and the hypogene mineralization occurs in the porphyries and adjacent andesites. These porphyries are north-northeast aligned and are cut by tourmaline–quartz–sulfide hydrothermal breccias. Prior to the onset of hyperarid conditions in the mid-Miocene (Alpers and Brimhall, 1988), the deposit underwent supergene alteration that produced a leached cap and enriched oxide (now dominated by atacamite and brochantite ($Cu_4(OH)_6SO_4$)) and sulfide (chalcocite, covellite, pyrite) zones overlying the primary (hypogene; chalcopyrite, bornite, molybdenite, tennanite, pyrite) sulfide zone (Fig. 2B). The leached cap forms an irregular surface covered by gravels, which vary in thickness from 30 to 180 m, thinning from north to south. A decline was constructed in the southern part of the deposit to obtain bulk samples of all zones, and there is local disturbance of the hydrology in this vicinity.

3. Methods

Details of the field sampling and laboratory methods have been presented elsewhere (Leybourne and Cameron, 2006). Briefly, groundwaters were collected from exploration drill holes at the Spence deposit in 1999

Fig. 2. A) Outline of the Spence deposit, showing the location of the major porphyries that intrude host andesitic volcanic rocks. Also shown are the locations of groundwater samples. Groundwater flow is generally NW to SE. B) The cross-section shows the southern part of the Spence deposit with atacamite and brochantite in the oxide zone, as well as supergene and hypogene sulfide zones.

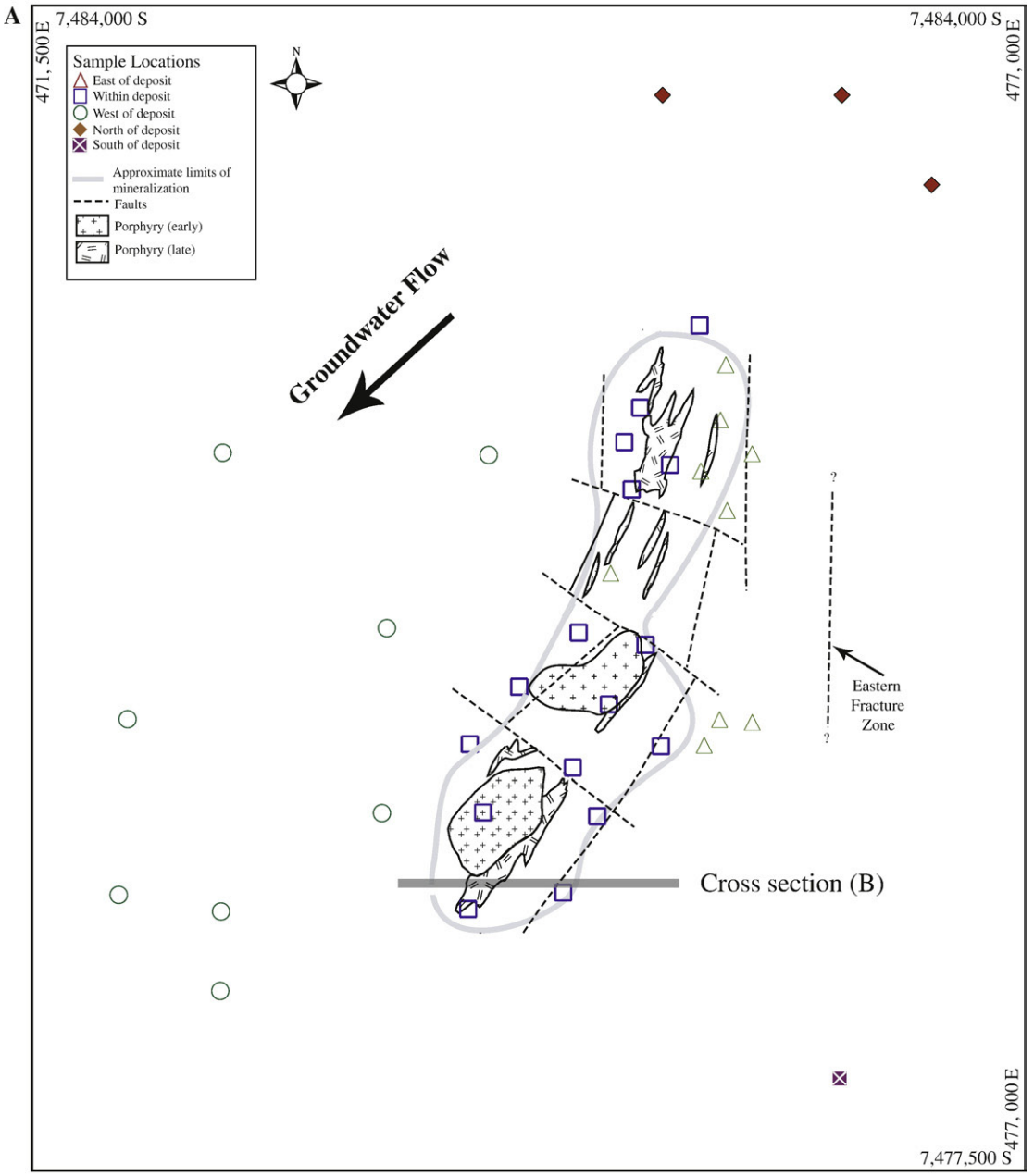
A
7,484,000 S
471, 500 E
477, 000 E
7,477,500 S
Sample Locations
East of deposit
Within deposit
West of deposit
North of deposit
South of deposit
Approximate limits of mineralization
Faults
Porphyry (early)
Porphyry (late)
N
Groundwater Flow
Eastern Fracture Zone
Cross section (B)

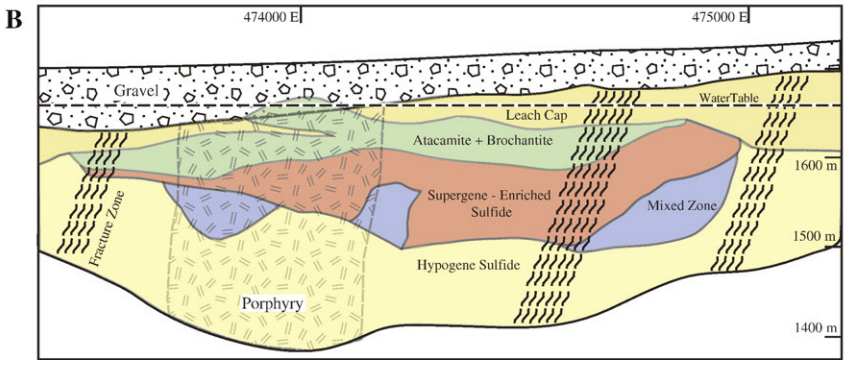
B
474000 E
475000 E
Gravel
WaterTable
Leach Cap
Atacamite + Brochantite
Supergene - Enriched Sulfide
Mixed Zone
Hypogene Sulfide
Porphyry
Fracture Zone
1600 m
1500 m
1400 m

Table 1
Geochemistry of Spence deposit groundwaters

Sample#	Area	Easting	Northing	TDS	pH	Eh (mV)	$\delta^{34}S_{CDT}$ (‰)	SO_4	As	Co	Cu	Mo	Pb	Re	Se	U	Zn
				mg/l				mg/l	µg/l	µg/l	µg/l	µg/l	µg/l	µg/l	µg/l	µg/l	µg/l
MLC00-1001	Within	474531	7480501	25,540	6.81	223	3.6	7031	25.6	65	443	83	0.2	5.27	197	0.39	95
MLC00-1002	Within	474531	7480501	25,280	6.75	−40	3.3	7049	26.4	64	389	87	1.11	5.28	192	0.42	77
MLC00-1004	Within	475040	7481435	24,918	7.52	−276	3.8	5686	42.6	5.61	148	475	0.27	30.71	185	1.86	65
MLC00-1009	Within	474990	7479868	21,374	7.46	−21	4.0	7313	17.9	43	1308	29	0.29	0.647	<50	1.89	1344
MLC00-1017	Within	474874	7481755	37,270	7.33	−259	2.9	5105	71.5	4.98	232	303	0.34	27.35	412	0.68	38
MLC99 1001	Within	474531	7480501	25,543	6.37	169	3.6	8709	19	97	1200	25	3.2	4	120	0.5	129
MLC99 1002	Within	474904	7480433	12,656	6.18	390	3.2	4913	12	9	490	9	1.1	3.7	<50	0.4	139
MLC99 1005	Within	475040	7481435		7.54	183	3.0	5282	19	4	363	354	0.2	16.1	189	<0.2	62
MLC99 1006	Within	474000	7479500	34,466	6.03	57	3.6	6273	46	2	121	222	0.8	0.5	169	<0.2	42
MLC99 1007	Within	474500	7479750	26,558	4.73	316	3.7	9503	43	187	28,991	3	4.1	13.9	308	1.8	212
MLC99 1010	Within	474445	7479053	29,162	5.08	0	3.4	7187	71	12	812	7	0.4	0.6	129	0.8	82
MLC99 1013	Within	474829	7481299	19,845	6.99	172	3.3	5012	29	10	88	38	2.6	6.6	98	1.8	37
MLC99 1014	Within	474787	7481564	38,410	7.25	190	2.4	7648	68	2	24	105	0.4	3.9	461	0.1	19
MLC99 1015	Within	474874	7481755	44,584	7.27	217	2.0	4916	95	3	10	263	0.1	5.6	706	0.7	5
MLC99 1016	Within	473916	7478963	27,000	7.3	152	2.9	9170	33	23	195	18	1.5	2.6	181	0.5	39
MLC99 1017	Within	473924	7479880	27,794	6.57	218	3.0	8850	16	50	191	5	1.6	0.5	84	0.8	134
MLC99 1018	Within	475208	7482214	43,105	7.35	235	2.1	9970	129	2	24	60	0.4	2.3	468	0.3	21
MLC99 1023	Within	474990	7479868	15,719	6.43	174	4.3	6102	<10	19	955	33	13.3	0.7	<50	0.3	723
MLC99 1024	Within	474990	7479868	16,008	6.43	174		6201	<10	29	2036	32	9.6	0.6	<50	0.3	1093
MLC99 1025	Within	474635	7479481	13,061	7.88			5656	<10	27	180	69	2.6	0.6	<50	0.2	49
MLC99 1026	Within	474200	7480200	24,409	9.22	−6	3.7	7918	10	2	14	221	0.1	1.5	51	<0.2	5
MLC99 1027	Within	474700	7480100	9359	7.54	66	7.8	4209	50	3	25	40	1.2	0.2	<50	<0.2	18
MLC00-1007	Within	475340	7481975	3875	8.3	−341	7.3	1387	3.7	1.66	20	4.08	0.41	0.214	2.64	0.05	13
MLC00-1020	West	472000	7480000	54,483	7.21	−186	3.5	1983	160.9	7.16	257	72	0.62	6.75	219	2.75	55
MLC00-1021	West	472000	7479000	20,114	7.87	−207	3.7	6648	38.3	19	79	190	0.33	1.64	130	2.41	45
MLC00-1023	West	473451	7479500	29,332	7.67	−165	3.7	7475	62.1	1.58	130	62	0.05	2.89	166	5.61	37
MLC00-1024	West	473451	7479500	29,165	7.67	−165		7490	60.8	1.66	128	63	0.07	2.95	162	5.51	40
MLC00-1003	West	473475	7480511	39,045	7.35	−338	2.5	4706	86.3	20	302	75	0.025	10.9	559	7.01	57

Table 1 (*continued*)

Sample#	Area	Easting	Northing	TDS	pH	Eh (mV)	$\delta^{34}S_{CDT}$ (‰)	SO_4	As	Co	Cu	Mo	Pb	Re	Se	U	Zn
				mg/l				mg/l	µg/l	µg/l	µg/l	µg/l	µg/l	µg/l	µg/l	µg/l	µg/l
MLC00-1014	West	473451	7479500	28,757	7.55	−278	3.4	7196	58.6	1.62	187	62	1.99	2.87	163	5.33	71
MLC00-1015	West	472500	7481500	145,020	6.53	−188	0.9	2004	278	10	564	90	0.48	11.1	486	2.52	131
MLC99-1003	West	473475	7480511	53,155	6.86	230	1.7	4269	93	4	13	63	1.1	8.6	797	0.3	35
MLC99-1004	West	474031	7481487	39,495	7.37	176	2.5	7001	73	2	14	24	0.2	5.1	503	<0.2	46
MLC99-1008	West	472549	7478950	27,594	7.28	485	2.5	5770	50	<2	13	66	0.1	2.1	330	<0.2	16
MLC99-1009	West	472521	7478522	26,761	7.41	470	2.8	6486	36	2	10	53	0.1	2.1	330	<0.2	14
MLC00-1005	East	475206	7481379	1716	8.39	−310	5.1	539	17.4	0.61	61	61	12.79	1.36	2.35	0.92	69
MLC00-1006	East	475206	7481379	1644	8.32	−254	5.2	533	17.6	0.54	67	60	13.18	1.31	2.1	0.9	74
MLC00-1008	East	475295	7480003	2237	8.21	−180	5.6	920	2.8	0.63	17	57	0.09	0.088	2.38	3.28	7.75
MLC00-1013	East	475500	7480000	24,073	7.81	−262	3.4	8847	31.5	4.19	127	14	0.025	2.44	111	0.71	88
MLC00-1016	East	475500	7481500	3087	8.67	−229	5.9	1096	7.4	0.74	27	7.95	0.41	0.503	2.68	0.46	9.02
MLC99-1011	East	475206	7481379	1412	7.57	125	4.5	524	28	<2	41	45	6.8	1.2	56	<0.2	30
MLC99-1012	East	475360	7481180	902	7.05	180	5.7	410	<10	2	127	9	0.1	0.1	<50	<0.2	80
MLC99-1019	East	475340	7481975	3395	7.97	-314	4.8	1378	<10	<2	9	15	1.2	0.1	<50	<0.2	19
MLC99-1020	East	475324	7481686		7.58	−48		3945	<10	3	53	2	2.8	0.9	<50	<0.2	58
MLC99-1021	East	475295	7480003	1900	7.14	160	5.1	920	<10	<2	29	54	5.1	0.1	<50	<0.2	5
MLC99-1022	East	475229	7479872	6377	7.78	31	4.7	2855	<10	4	12	136	23.8	0.7	<50	<0.2	84
MLC99-1029	East	474708	7480838	2238	7.32	88	3.6	1204	<10	<2	48	33	4.8	0.5	<50	<0.2	17
MLC00-1010	North	476000	7483500	27,351	7.71	−228	3.4	8721	87.3	1.33	121	28	0.025	0.987	78	11.98	39
MLC00-1011	North	476500	7483000	29,478	7.86	−288	3.4	10,045	119.3	1.68	126	38	0.025	0.795	60	13.58	44
MLC00-1012	North	475000	7483500	32,973	8.1	−314	3.6	9940	45	1.8	113	19	0.17	0.101	<50	18.46	35
MLC00-1022	South	475977	7478000	34,434	7.52	−131	3.1	7256	72.5	1.75	154	65	0.025	3.39	211	18.85	34

and 2000, using flow-through bailer and down-hole pump methods, respectively. Water samples were tested *in situ* for pH, Eh, electrical conductivity (as a measure of salinity), temperature and dissolved oxygen (DO) using a Hydrolab Quanta multiprobe meter. The pH was temperature compensated and was calibrated at least daily using NIST traceable pH 4, 7 and 10 buffers. We did not attempt to compensate for the influence of high ionic strength on pH for the most saline groundwaters recovered (pmH scale) (Bates and Culberson, 1977). Gieskes et al. (1991) found differences between the standard pH and pmH scales of around 0.114±0.013 pH units for waters from the Nankai Trough; differences at this level for the more saline Spence groundwaters do not affect the interpretations presented here. Both filtered (to 0.45 µm using Sterivex capsule filters) and unfiltered aliquots were collected for cation analysis and were acidified to 1% by volume with ultrapure HNO_3. Major cations were analyzed by inductively coupled plasma optical emission spectrometry (ICP-OES; PE

Table 2
Spearman rank correlation matrix for Spence deposit groundwaters

	pH	Eh	DO	$\delta^{18}O_{VSMOW}$	$\delta^{34}S_{CDT}$	TDS	HCO_3	Cl	SO_4	Br	I	Ca	Mg	Na	K	Si	B	Fe	Mn
pH	1																		
Eh	−0.65	1																	
DO	−0.34	0.52	1																
$\delta^{18}O_{VSMOW}$	−0.33	0.14	−0.02	1															
$\delta^{34}S_{CDT}$	0.44	−0.35	−0.18	−0.85	1														
TDS	−0.33	0.09	−0.05	0.96	−0.81	1													
HCO_3	0.72	−0.56	−0.27	−0.45	0.56	−0.45	1												
Cl	−0.40	0.14	−0.04	0.95	−0.80	0.95	−0.54	1											
SO_4	−0.13	0.13	0.02	0.52	−0.44	0.52	−0.08	0.41	1										
Br	−0.38	0.09	−0.03	0.85	−0.71	0.87	−0.53	0.91	0.38	1									
I	−0.37	0.23	0.11	0.82	−0.78	0.83	−0.57	0.82	0.46	0.89	1								
Ca	−0.50	0.24	0.01	0.89	−0.81	0.88	−0.64	0.96	0.34	0.86	0.77	1							
Mg	−0.35	0.04	−0.07	0.94	−0.78	0.97	−0.46	0.95	0.49	0.88	0.80	0.89	1						
Na	−0.36	0.12	−0.04	0.96	−0.80	0.99	−0.45	0.96	0.53	0.88	0.81	0.90	0.96	1					
K	−0.51	0.21	−0.05	0.84	−0.70	0.81	−0.49	0.86	0.44	0.78	0.67	0.86	0.81	0.84	1				
Si	−0.21	0.23	0.34	0.33	−0.36	0.26	−0.29	0.22	0.34	0.13	0.26	0.28	0.23	0.22	0.27	1			
B	−0.21	0.03	−0.16	0.83	−0.70	0.75	−0.31	0.75	0.65	0.63	0.70	0.69	0.74	0.74	0.71	0.33	1		
Fe	−0.20	0.35	0.35	−0.25	0.20	−0.28	0.02	−0.15	−0.52	−0.06	−0.16	−0.07	−0.27	−0.26	−0.07	0.03	−0.50	1	
Mn	−0.37	0.12	−0.04	−0.29	0.25	−0.24	−0.02	−0.16	−0.12	−0.11	−0.28	−0.09	−0.22	−0.21	0.10	−0.16	−0.27	0.39	1
Al	−0.05	−0.35	−0.24	0.20	−0.05	0.20	−0.09	0.22	0.09	0.18	0.16	0.17	0.25	0.14	0.21	0.26	0.36	−0.14	−0.06
Ba	0.20	−0.46	−0.51	0.06	0.11	0.08	0.15	0.14	−0.31	0.14	−0.05	0.13	0.10	0.05	0.21	−0.13	0.02	0.30	0.35
Cs	−0.42	−0.09	−0.14	0.45	−0.33	0.53	−0.24	0.47	0.57	0.46	0.41	0.41	0.57	0.54	0.50	−0.02	0.46	−0.26	0.25
Ni	−0.46	0.04	−0.26	0.50	−0.35	0.48	−0.39	0.53	0.39	0.49	0.38	0.53	0.54	0.50	0.63	0.05	0.61	−0.30	0.25
Li	−0.48	0.22	0.02	0.90	−0.74	0.90	−0.49	0.90	0.57	0.79	0.74	0.86	0.88	0.92	0.88	0.21	0.75	−0.23	−0.09
Rb	−0.60	0.15	−0.01	0.69	−0.59	0.70	−0.44	0.70	0.61	0.64	0.57	0.67	0.73	0.73	0.81	0.19	0.64	−0.12	0.22
Sr	−0.23	0.06	−0.16	0.93	−0.80	0.93	−0.47	0.93	0.46	0.84	0.78	0.90	0.93	0.93	0.76	0.23	0.78	−0.36	−0.36
U	0.13	−0.46	−0.24	0.30	−0.15	0.34	0.15	0.25	0.36	0.20	0.11	0.19	0.37	0.34	0.20	0.04	0.41	−0.62	−0.19
V	0.20	−0.50	−0.48	0.39	−0.14	0.36	0.06	0.37	0.13	0.32	0.21	0.30	0.43	0.34	0.18	−0.05	0.49	−0.52	−0.32
As	−0.22	0.00	0.01	0.85	−0.69	0.87	−0.33	0.82	0.40	0.74	0.75	0.77	0.84	0.84	0.61	0.30	0.69	−0.22	−0.42
Co	−0.57	0.29	−0.06	0.30	−0.30	0.29	−0.45	0.34	0.43	0.35	0.30	0.40	0.30	0.33	0.57	0.09	0.41	−0.18	0.52
Cr	0.21	−0.19	−0.11	0.62	−0.49	0.58	−0.20	0.57	0.29	0.45	0.57	0.49	0.58	0.53	0.25	0.24	0.67	−0.54	−0.66
Cu	−0.45	−0.06	−0.14	0.17	−0.07	0.16	−0.15	0.18	0.37	0.19	0.11	0.18	0.21	0.19	0.43	0.00	0.34	−0.32	0.39
Mo	−0.02	−0.07	−0.20	0.40	−0.27	0.36	−0.35	0.47	−0.07	0.41	0.31	0.51	0.40	0.36	0.33	−0.15	0.36	−0.10	−0.10
Pb	−0.16	0.17	0.17	−0.43	0.33	−0.43	0.13	−0.41	−0.33	−0.31	−0.33	−0.35	−0.48	−0.42	−0.19	−0.25	−0.49	0.73	0.43
Re	−0.37	0.13	0.12	0.63	−0.62	0.56	−0.51	0.64	0.21	0.55	0.55	0.69	0.58	0.56	0.63	0.26	0.66	−0.16	−0.13
Se	−0.49	0.33	0.12	0.88	−0.83	0.83	−0.66	0.88	0.37	0.78	0.77	0.89	0.83	0.83	0.77	0.35	0.77	−0.22	−0.26
Zn	−0.35	0.02	0.08	0.02	−0.01	0.01	−0.11	0.04	0.24	0.11	0.10	0.02	0.03	0.02	0.22	−0.08	0.18	−0.05	0.38

Data from Table 1 and from Leybourne and Cameron (2006).

Optima 3300 DV), trace elements by mass spectrometry (ICP-MS; PE-Sciex Elan 6100 DRC), anions by ion chromatography (Dionex DX 600) and ICP-OES (sulfur), and alkalinity by end-point titration. Elemental analyses were performed at the Geological Survey of Canada (waters collected in 1999) and the Geochemistry Laboratories at the University of Texas at Dallas (waters collected in 2000). Electrical balances are excellent with all waters reported here having less than 5% difference between cations and anions. For ICP-MS analyses, measurements were made using external calibration. A drift standard was measured after every five unknowns and the data drift corrected following a modification of the method of Cheatham et al. (1993). Typical ICP-MS operating conditions were 1100 W forward RF power, 13 l/min plasma gas flow, 1.2 l/min auxiliary gas flow and typically around 0.92 l/min nebulizer gas flow. Nebulizer gas flow rates were optimized daily to minimize oxide formation (CeO^+) and double ionization (Ba^{++}). Sample uptake rate was 1 ml/min. Se was measured using the least interfered isotopes, ^{78}Se and ^{82}Se. Detection limits for As are elevated owing to the potential for mass overlap on ^{75}As through the formation of $^{40}Ar^{35}Cl^+$ in the plasma. For Re analyses, both isotopes (^{185}Re and ^{187}Re) were monitored and samples from 1999 were rerun at the UTD laboratories, with excellent agreement between the labs. Saturation indices and P_{CO2} calculations were performed using the computer code

Al	Ba	Cs	Ni	Li	Rb	Sr	U	V	As	Co	Cr	Cu	Mo	Pb	Re	Se	Zn
1																	
0.26	1																
0.26	0.02	1															
0.48	0.27	0.59	1														
0.12	−0.03	0.57	0.56	1													
0.29	0.07	0.84	0.71	0.81	1												
0.21	0.10	0.37	0.50	0.82	0.58	1											
0.51	−0.02	0.34	0.42	0.28	0.33	0.34	1										
0.54	0.27	0.19	0.51	0.22	0.19	0.49	0.61	1									
0.24	0.02	0.42	0.37	0.71	0.55	0.83	0.45	0.47	1								
0.18	0.09	0.57	0.72	0.42	0.66	0.28	0.07	0.00	0.08	1							
0.37	0.04	0.12	0.20	0.43	0.19	0.67	0.37	0.61	0.68	−0.21	1						
0.47	0.02	0.60	0.65	0.30	0.63	0.11	0.46	0.23	0.10	0.65	−0.16	1					
0.06	0.21	0.05	0.28	0.30	0.08	0.48	0.13	0.40	0.40	0.02	0.38	−0.06	1				
−0.18	0.11	−0.19	−0.11	−0.32	−0.18	−0.52	−0.43	−0.43	−0.48	0.08	−0.64	0.03	−0.14	1			
0.47	0.07	0.28	0.61	0.52	0.50	0.61	0.32	0.39	0.59	0.42	0.42	0.33	0.45	−0.14	1		
0.16	−0.04	0.34	0.49	0.78	0.61	0.86	0.13	0.29	0.78	0.35	0.54	0.10	0.48	−0.37	0.76	1	
0.33	0.03	0.45	0.58	0.15	0.44	−0.03	0.23	0.08	−0.06	0.57	−0.14	0.72	−0.07	0.21	0.26	−0.01	1

PHREEQC (Parkhurst and Appelo, 1999), utilizing the WATEQ4F thermodynamic database (Ball and Nordstrom, 1991). Samples with salinities greater than seawater are excluded from discussion of saturation for Cu species because the method for activity coefficient is not valid at these ionic strengths.

4. Results

4.1. Groundwater trace metal and metalloid concentrations

Selenium concentrations vary from 2 to 800 μg/l (Table 1). Selenium concentrations in groundwaters along the eastern margin of the deposit are the lowest in the study (e.g., most are between 2 and 3 μg/l; one more saline water at 110 μg/l), whereas the highest Se concentrations occur in the northern section of the deposit and down-flow from the northern section. Selenium displays strong positive correlations with oxygen isotopes ($r=0.873$; Spearman Rank correlation, Table 2), As ($r=0.776$) (Fig. 3), and TDS ($r=0.840$). Note, r-values are statistically significant at the >99.9% confidence interval ($p<0.001$) unless otherwise noted. Additionally, Se concentrations increase as the sulfur isotopic compositions become lighter, suggesting that elevated Se concentrations are derived from Spence deposit sulfide minerals (see below). Selenium shows poor inverse relationships with Fe, Mn, Zn, and Pb (e.g., Pb shown on Fig. 3). Additionally, Se/TDS ratios

increase with increasing Se concentration indicating that Se concentrations increase more rapidly than does TDS, or conservative tracers such as Na (Fig. 4).

Groundwaters along the eastern margin of the deposit have generally low Re concentrations (≤ 1 μg/l; Fig. 5), whereas groundwaters within the deposit, in particular

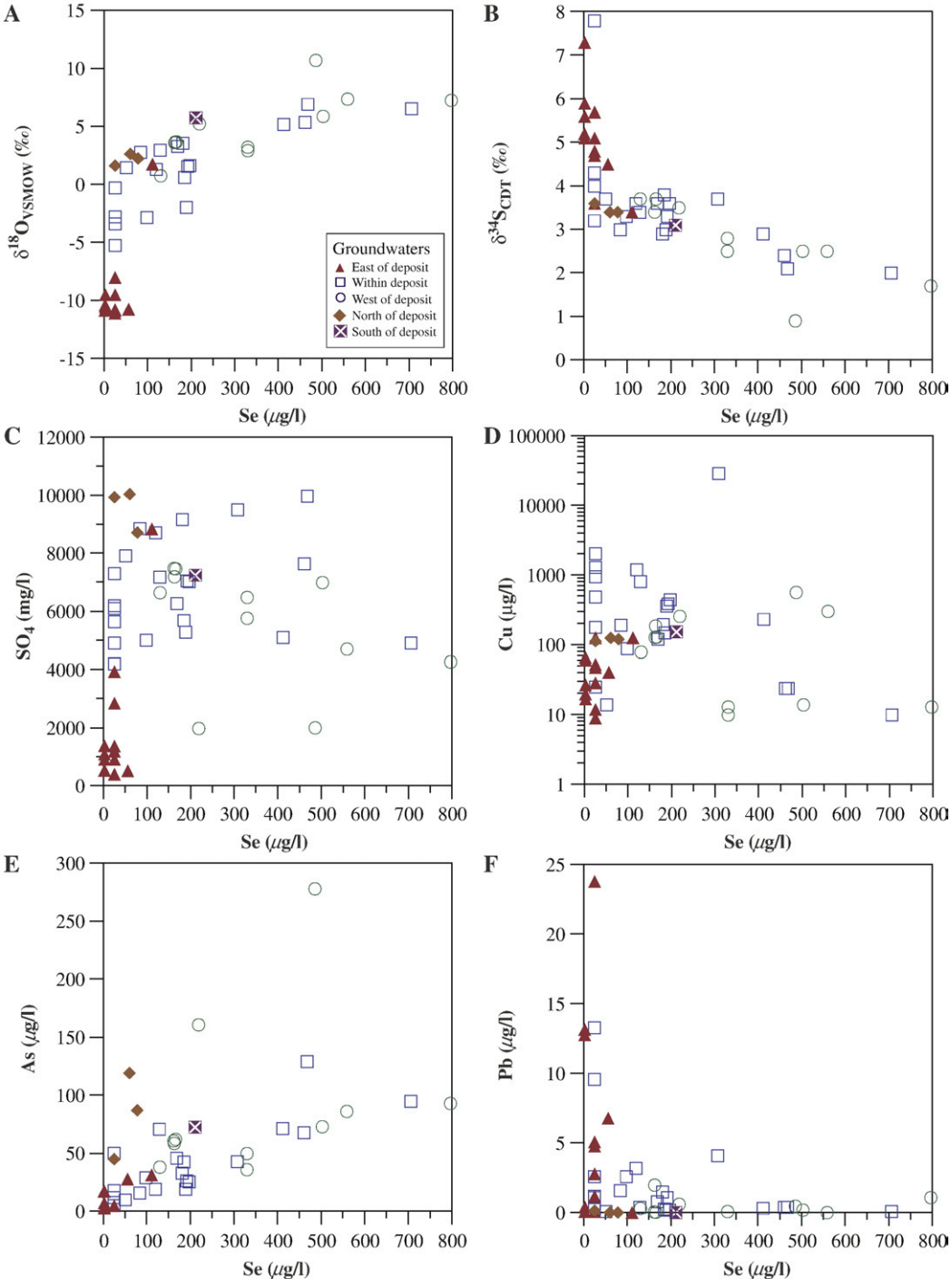

Fig. 3. Variation diagrams illustrating the relationships between dissolved Se and other porphyry–copper related elements and isotopes for Spence groundwaters.

the northern half, and down-flow of the deposit have elevated Re concentrations, up to 30.7 μg/l (Fig. 5). Rhenium shows a general increase with increasing TDS ($r=0.562$, $p=0.0167$) and with increasing Se ($r=0.760$, $p=0.0014$; Fig. 5), whereas there is no consistent relationship between Re and Cu or Mo.

Arsenic concentrations are variable, ranging from <5 to 278 μg/l (Figs. 3E, 5C). Similar to Se and Re, As concentrations are generally low in waters that flow in from the east and increase into and down-flow of the deposit. Arsenic concentrations increase with increasing salinity and show a positive correlation with Se concentrations (Fig. 3E).

Molybdenum concentrations are variable along the eastern margin of the deposit, ranging from 2 to 136 μg/l compared to 5 to 475 μg/l for groundwaters within the deposit (Fig. 5E). Within the deposit, Mo concentrations are highest in the northern segment and along the southwestern edge of the deposit. Down-flow to the west and southwest, Mo concentrations are generally lower than within the deposit (24–190 μg/l).

Copper concentrations are highly variable, ranging from 9 to 2036 μg/l (Figs. 3D, 5F). One sample, recovered from the exploration decline has a Cu concentration of 29,000 μg/l; this sample is not considered in the discussion below. The most elevated Cu concentrations occur in groundwaters within the deposit, especially in the central portion, although groundwaters along the eastern margin have Cu concentrations up to 127 μg/l. Waters down-flow of the deposit have consistently low Cu concentrations of 10–14 μg/l.

4.2. Filtered versus unfiltered trace element concentrations

Both filtered and unfiltered aliquots were collected for cation determination (Fig. 6). Arsenic ($H_2AsO_4^-$, $HAsO_4^{2-}$), Mo ($HMoO_4^-$), Re (ReO_4^-) and Se ($HSeO_3^-$, SeO_4^{2-}, SeO_3^{2-}) behave as oxyanions (Brookins, 1988) or as neutral aqueous species ($As(OH)_{3(aq)}$) at the Eh and pH conditions of the waters sampled at the Spence deposit (e.g. Se, As; Fig. 7). These elements for the most part show identical compositions between filtered and unfiltered aliquots, with As showing the greatest difference (Fig. 6). In contrast, Fe, Mn and Al are strongly controlled by the suspended sediment phase, with significant differences between the filtered and unfiltered aliquots (Fig. 6). For the Spence deposit groundwaters, metals that show moderate to major fractionation onto suspended material, including colloids, include Cu, Pb, and Zn and to a lesser extent, Co and Cd (i.e. the affinity for colloids increases in the order Cd<Co<Zn<Cu<Pb) (Fig. 6). Note also that for the metal cations, the standard deviation (variability) in the difference between filtered and unfiltered is much greater than for the oxyanions (Fig. 6).

5. Discussion

5.1. Origin of Spence groundwaters

Major ion concentrations and stable isotope (O, H, C, and S) ratios of Spence deposit groundwaters were reported by Leybourne and Cameron (2006). In order to

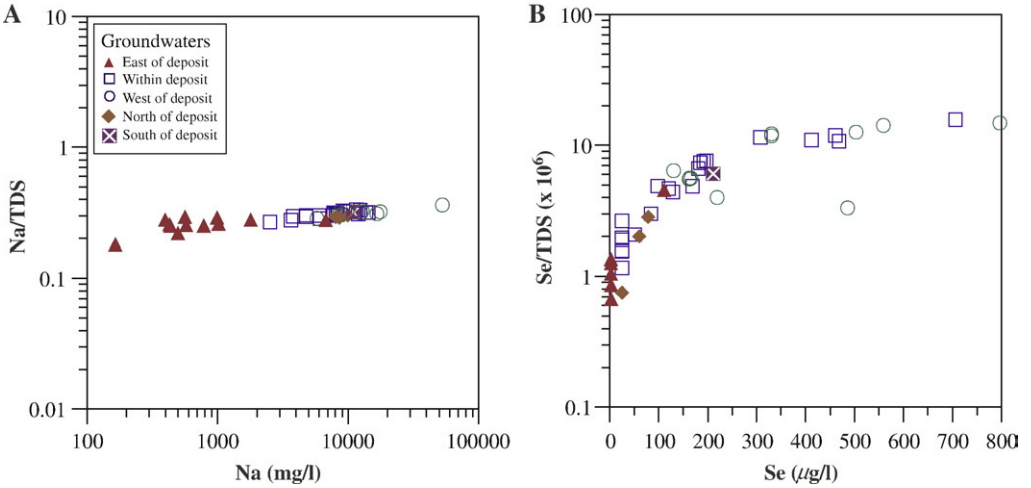

Fig. 4. Variation diagrams showing a porphyry–copper related elements (Se) and a conservative tracer (Na) normalized to salinity (TDS). Note that porphyry-related metal and metalloid concentrations (e.g., Se) increase at a greater rate than salinity (increasing metal/TDS ratios with increasing metal), whereas Na displays an essentially flat trend (increase is generally equal to the increase in salinity).

properly interpret the trace metal and metalloid geochemistry, some comments on this previous work are warranted. Based on variations in major ion chemistry and the $\delta^{18}O_{VSMOW}$ and $\delta^{2}H_{VSMOW}$ ratios, there appear to be two dominant sources of water at the Spence deposit. Groundwaters up-flow of the

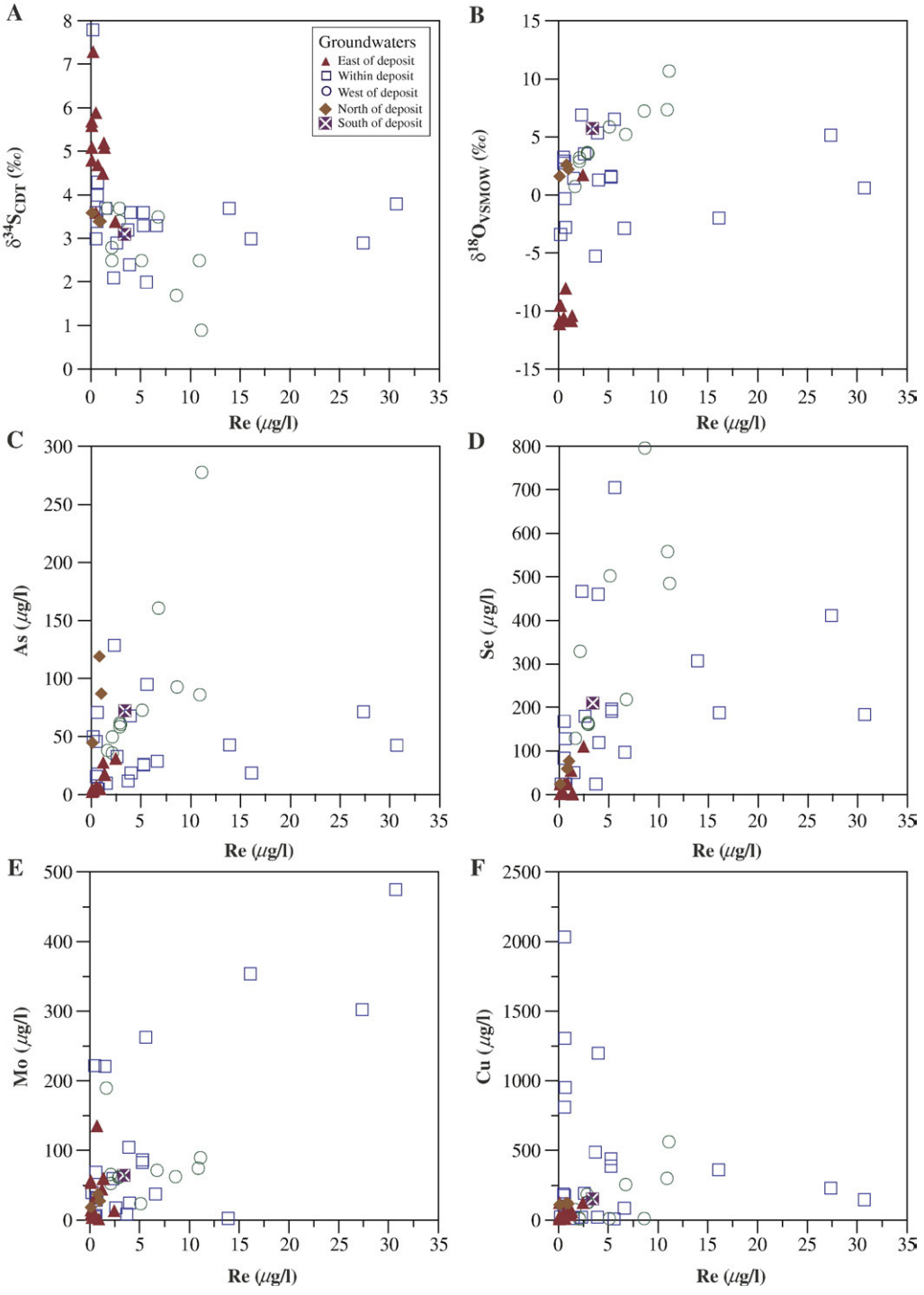

Fig. 5. Variation diagrams illustrating the relationships between dissolved Re and other porphyry–copper related elements and isotopes for Spence groundwaters.

deposit are characterized by low salinities (typically <10,000 mg/l) and the $\delta^{18}O_{VSMOW}$ and $\delta^{2}H_{VSMOW}$ ratios are consistent recharge in the high Andes (>4000 m elevation); thus these waters are interpreted as regional meteoric waters. In contrast, groundwaters within and down-flow of the deposit have elevated salinities (most ≤ seawater in ionic strength; two samples > seawater), and the $\delta^{18}O_{VSMOW}$ and $\delta^{2}H_{VSMOW}$ ratios are consistent with mixing of meteoric waters with basinal brines. Sulfur isotope ratios are also variable (Leybourne and Cameron, 2006); groundwaters up-flow of the deposit have heavier sulfur isotope ratios (+4 to +8‰ $\delta^{34}S_{CDT}$), similar to regional waters and salars (Carmona et al., 2000; Pueyo et al., 2001; Rech et al., 2003), whereas groundwaters within and down-flow of the deposit have progressively lighter sulfur isotope ratios (+1 to +4‰ $\delta^{34}S_{CDT}$), approaching porphyry copper ore values (Field and Gustafson, 1976; Dold and Spangenberg, 2002).

5.2. Comparisons with seawater and groundwater in other settings

Groundwaters in and around the Spence porphyry copper deposit have elevated Se (up to 800 μg/l), Re (up to 31 μg/l), Mo (up to 475 μg/l) and As (up to 300 μg/l) concentrations compared to up-flow (regional) waters (Figs. 3–5). Although these metal and metalloid concentrations in the groundwaters in the deposit are clearly anomalous compared to the regional meteoric waters, how do they compare to other groundwater systems and seawater?

Spence deposit groundwaters have elevated Re concentrations compared to low temperature fluids in other settings. Seawater Re concentration is around 7.3 ng/l (Anbar et al., 1992). Groundwaters from the southern Great Basin, Nevada, have average Re concentrations of 6.9 ng/l, with a range of 1.3 to 26.1 ng/l (Hodge et al., 1996). Dalai et al. (2002) reported Re concentrations from rivers in the Himalayas, with elevated values derived from weathering of black shales, with values up to 20.7 ng/l, three order of magnitude lower than Spence deposit groundwaters. Thus, the Re concentrations of Spence deposit groundwaters are anomalous, reaching values typically only recorded in anoxic environments (Crusius et al., 1996; Jaffe et al., 2002).

Seawater has an average Mo concentration of around 10.6 μg/l (Sohrin et al., 1999), similar to many Spence groundwaters, but well below the most elevated waters from within the deposit (Fig. 5E). There are relatively few studies of Mo in groundwater systems. Hodge et al. (1996) reported groundwater Mo concentrations from Nevada of 6.3 to 25 μg/l (average 11.5 μg/l). Groundwaters associated with undisturbed volcanogenic massive sulfide (VMS) mineralization in eastern Canada have groundwater Mo concentrations from 0.7 to 56 μg/l (Leybourne et al., 1998). Spence deposit groundwaters range up to much higher Mo concentrations.

Although Se commonly substitutes for S in sulfide minerals in VMS systems (Layton-Matthews et al., in press), groundwaters associated with disturbed and undisturbed VMS deposits generally have low Se concentrations, typically less than 10 μg/l (Leybourne and Goodfellow, 2003; Phipps et al., 2004). Selenium concentrations on the same order as at the Spence deposit have been reported from the upper Colorado River basin (up to 1300 μg/l) (Engberg, 1999) and from shallow wells in the Sierra Nevada alluvial aquifer where Se ranges from <1 to 2000 μg/l (Deverel et al., 1994).

There have been numerous studies of As in terrestrial aqueous systems (Smedley and Kinniburgh, 2002), and arsenic contamination of water supplies from natural (geogenic) and anthropogenic (mining) sources in northern Chile is a known health issue (Romero et al., 2003; Caceres et al., 2005; Christian et al., 2006; Oyarzun et al., 2006). A study of As in the Rio Loa system of northern Chile reported elevated values as high as 27,000 μg/l in a tributary draining the El Tatio geothermal system (Romero et al., 2003). Arsenic in groundwaters associated with ore deposits are typically elevated compared to background values and Spence

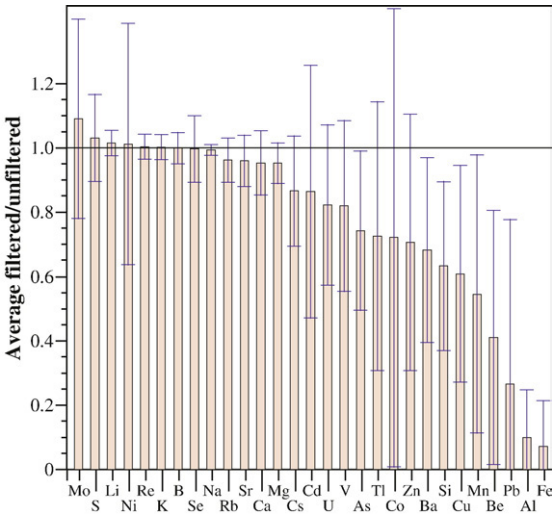

Fig. 6. Bar chart showing average elemental values for the filtered/unfiltered aliquots. The error bars represent the standard deviation for each element. Note that Se and Re show essentially no difference between the filtered and unfiltered aliquots, whereas metals such as Fe and Al, strong colloid formers, occur largely as suspended matter.

deposit groundwaters have As values similar to groundwaters associated with ore deposits elsewhere (Clark and Raven, 2004; Phipps et al., 2004).

5.3. Source of Re, Se, Mo, As in Spence deposit groundwaters

Several lines of evidence suggest that the elevated Cu, Se, Re, As, and Mo concentrations in groundwaters within and down-flow of the deposit are the result of water–deposit interaction superimposed on mixing of meteoric and saline groundwaters. These include: 1) the fact that low salinity waters up-flow of the deposit generally have low abundances of Re, Se, As, and Mo, 2) that groundwaters in the deposit are anomalous in metals and metalloids that are characteristic of porphyry copper mineralization, in particular Re and Mo, and 3) the correlation between these trace metalloids and sulfur isotopes (Figs. 3B, 5A). Thus, the source of anomalous metal and metalloid concentrations in the Spence groundwaters is interpreted to be hypogene and/or supergene sulfides in the Spence porphyry copper deposit.

Molybdenum is common in porphyry copper systems, and is hosted primarily in molybdenite. For example, Mo and As reach concentrations in excess of 0.1 wt.% in whole rock assay samples at the Chuquicamata deposit,

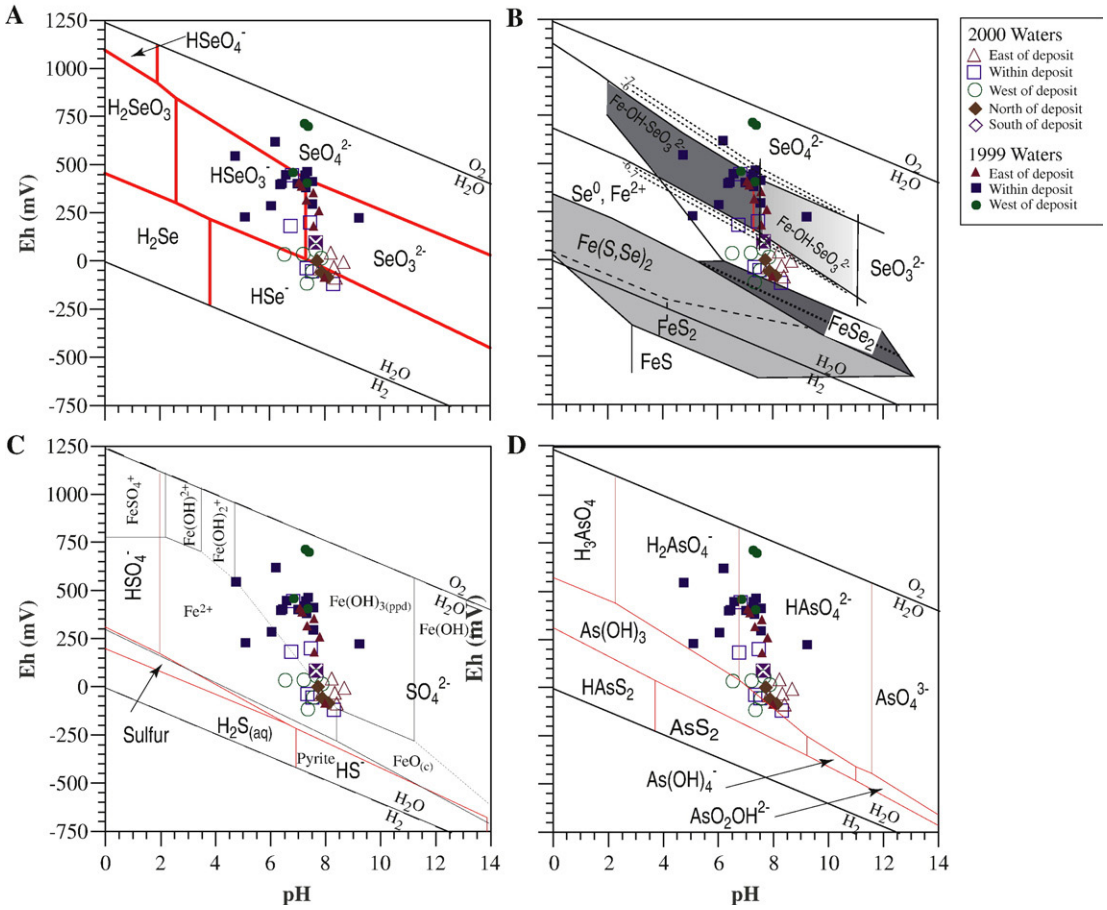

Fig. 7. Eh versus pH plots for Spence groundwaters, showing speciation of Se, SO_4 and As. Note that the samples collected in 2000 (down-hole pump) have generally lower Eh values than the 1999 (flow-through bailer) samples. A) Se speciation, with $[Se]=10^{-6}$, $[SO_4]=10^{-2}$, $[HCO_3]=10^{-3}$, $[Fe]=10^{-4}$. The formation of Se solids (native Se, $FeSe_2$ and FeSe) was suppressed. B) Selenium speciation diagram after Howard (1977). Dotted line within the ferroselite field ($FeSe_2$) is the $FeSe_2/Fe_2O_3$–Se^0 boundary. The dashed line within the pyrite field indicates the Se^0–H_2Se and Se^0–HSe^- couples. The dashed lines parallel to the selenate and selenite fields indicates displacement of the field owing to adsorption of Se on Fe-oxides. The shaded field Fe–OH–SeO_3^{2-} indicates conditions of strong adsorption; adsorption decreases with increasing pH. $[Se]=10^{-5}$, $[SO_4]=10^{-1}$, $[Fe]=10^{-3}$. C) SO_4 speciation, with $[SO_4]=10^{-2}$, $[HCO_3]=10^{-3}$, $[Cl]=10^{-1}$. Also shown are the fields for Fe speciation. D) As speciation, with $[As]=10^{-6}$, $[SO_4]=10^{-2}$, $[HCO_3]=10^{-3}$, $[Fe]=10^{-5}$. For the As diagram, formation of realgar, orpiment, scorodite and claudetite was suppressed, as they are kinetically unlikely to form in these waters. For the Fe diagram, magnetite, hematite and goethite were suppressed. Plots A, C, and D were created using The Geochemists Workbench (Bethke, 1994).

close to the West Fault (Ossandon et al., 2001). There has been relatively little research into Se and Re concentrations of porphyry–Cu deposits, with the exception of the use of the Re–Os method of dating sulfide deposits (Freydier et al., 1997; Mathur et al., 2000) and laser ablation analyses of sulfide inclusions in samples of hornblende diorite from porphyry systems (Audétat and Pettke, 2006). Rhenium is a characteristic trace element in porphyry copper deposits (Cameron et al., 2000), and is primarily hosted in molybdenite (McCandless et al., 1993), in which ReS_2 forms a solid solution with MoS_2 (Morris, 1969). Freydier et al. (1997) studied Re–Os isotopic systematics in sulfide minerals from two Chilean porphyry deposits and found Re concentrations of chalcopyrite, sphalerite, bornite and pyrite from the El Teniente deposit range from 0.053 to 0.18 ppb, whereas in pyrite from the Andacollo deposit, Re concentrations reach 100 ppb. Mathur et al. (2000) carried out a similar study on seven porphyry–Cu deposits in Chile and showed data for pyrite and chalcopyrite with Re concentrations ranging from 0.17 to 46.5 ppb.

Although selenium minerals have been observed in many different styles of mineralization (e.g., epithermal deposits, skarn deposits, sandstone- and unconformity-type uranium deposits), Se is mostly present as a solid solution impurity in hypogene sulfide minerals (Xiong, 2003a). The substitution of Se for S in sulfides is a result of their similar size and oxidation state (Simon et al., 1997). Discrete selenide phases are not typical of porphyry copper systems, such as those of northern Chile, presumably because during hypogene mineralization, reduced sulfur activities are high, so that $fSe_{2(g)}/fS_{2(g)}$ ratios are too low to stabilize selenide minerals (Simon and Essene, 1996; Simon et al., 1997).

During supergene weathering of porphyry copper deposits, sulfide minerals are progressively oxidized and their constituents redistributed according to their behavior as a function of the redox state and pH of the system (Thornber, 1975; Alpers and Brimhall, 1988). Although considerable attention has been given to the fate of Cu during supergene oxidation, there is little information regarding Se, Re, or Mo. Given that the groundwaters at the Spence deposit are likely interacting with both the hypogene and supergene parts of the deposit, some comments are warranted.

As hypogene sulfides are oxidized during supergene processes, Cu is removed in solution and reprecipitates lower in the supergene profile where conditions are more reducing. In the Atacama Desert, Cu is reprecipitated in the oxide zone as carbonates (e.g., malachite; $Cu_2(OH)_2CO_3$), chlorides (e.g., atacamite), sulfates (e.g., brochantite, antlerite ($Cu_3(OH)_6SO_4$), chalcanthite ($Cu_3SO_4{\cdot}5H_2O$)), oxides and copper wad (Mn oxyhydrates) (Münchmeyer, 1996; Mote et al., 2001). Regarding the fate of the other species, we can draw analogies with sulfide weathering in other systems and climates. Molybdenum and Se are immobile under acidic oxidizing conditions and thus may be retained along with As and Sb as in the Bathurst Camp (Boyle, 2003). In supergene zones developed on porphyry copper deposits in the western U.S., molybdenite or ferrimolybdite ($Fe_2(MoO_4)_3{\cdot}nH_2O$) are the dominant Mo minerals present (McCandless et al., 1993). During supergene alteration, some molybdenites were found to have experienced some Re loss, with ferrimolybdite at the Questa Mine, New Mexico, containing no Re (McCandless et al., 1993). However, Re was enriched in secondary minerals, some intergrown with molybdenite, such as illite and powellite ($Ca(Mo,Re)O_4$) (McCandless et al., 1993). In the presently neutral to alkaline pH and redox and salinity conditions of the Spence deposit groundwaters (Fig. 7), Mo is mobile. Hodge et al. (1996) concluded that Mo in groundwaters in the Great Basin of Nevada and California behaved conservatively, similar to its behavior in seawater. As discussed below, in northern Chile groundwaters, Mo also appears to be conservative relative to Se and Re.

Spence groundwaters have significantly lower U/Re ratios than groundwaters from Nevada. Hodge et al. (1996) determined U/Re ratios for groundwaters from Ash Meadows and Death Valley of between 230 and 1800 from an aquifer system in Nevada, U.S.A. In contrast, most groundwaters around, within and down-flow of the Spence deposit have U/Re <10 (Fig. 8). Rhenium is present within porphyry copper mineralization, whereas U is not. Thus, these data are consistent with our contention that the anomalous metal and metalloid concentrations in Spence deposit groundwaters are derived from mineralization rather than the host rocks.

5.4. Speciation and attenuation of Re, Mo, Se, As in Spence deposit groundwaters

The speciation and transport of metals and metalloids away from porphyry copper mineralization is important both in terms of understanding the fate and transport of these species in the secondary environment, and for understanding the development of geochemical anomalies in surface horizons in arid environments, of concern to mineral exploration. We have shown in this study that some porphyry-related species, such as Se, Re, Mo, and As appear to remain in solution for some distance down-flow of the Spence deposit. We suggest that the primary reason that As, Se, Re and Mo concentrations of

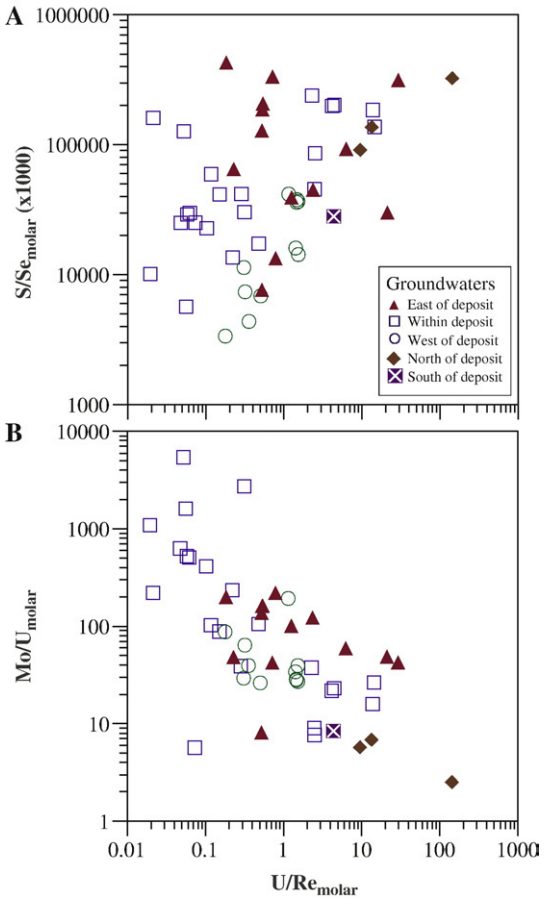

Fig. 8. Plots of A) Se/S$_{molar}$ and B) Mo/U$_{molar}$ versus U/Re$_{molar}$ for Spence deposit groundwaters.

groundwaters remained elevated down-flow of the deposit, whereas Cu and other base metals decrease rapidly down-flow, is that the former elements are speciated primarily as neutral species or oxyanions in these groundwaters. All the groundwaters recovered to date from the Spence deposit have Eh–pH values in which As, Se, Re, and Mo are speciated either as oxyanions or as neutral hydroxides (e.g., As and Se; Fig. 7). Additionally, no sulfides are stable, as all the waters are in the SO_4 stability field (Fig. 7C). Note that the Eh measurements on the Spence groundwaters were made with a Pt electrode, so that the measurements most likely reflect the Fe^{II}/Fe^{III} redox couple (Runnells and Lindberg, 1990), consistent with the samples collected by down-hole pump straddling the $Fe^{2+}/Fe(OH)_{3(ppd)}$ phase boundary (Fig. 7C). Thus, probably the most important constraint on attenuation of As, Se, Re, and Mo in Spence groundwaters is adsorption to mineral surfaces.

Species that form oxyanions in solutions have variable tendencies to adsorb to the surfaces of metal oxyhydroxides, roughly inversely proportional to their dissociation constant in oxidizing waters at neutral to alkaline pH (Johannesson et al., 1996). Tachi et al. (1998) found that Se(IV) was most strongly adsorbed by Fe-oxyhydroxides and pyrite at pH values <8 in tuff samples, consistent with the pH_{znpc} (znpc = zero net proton charge) of $Fe(OH)_3$ ranging from 8.5 to 8.8 (Langmuir, 1997). Similarly, Se(IV) adsorption on clays (smectite) was found to be significant only at pH <5 (Boult et al., 1998). Se(IV) is more strongly adsorbed than Se(VI), and in the presence of hydrous Fe-oxides, Se(IV) displays a strong adsorption edge at pH 8.5, whereas, Se(VI) has a strong adsorption edge at pH ~6 (Plant et al., 2003). However, the adsorption edge for Se(IV) shifts to lower pH as the concentration of amorphous Fe-oxyhydroxides decreases and as the concentration of competing anions, including sulfate, increases (Balistrieri and Chao, 1990; Kent et al., 1994; Kent et al., 1995). Yllera de Llano et al. (1996) showed, using X-ray adsorption near edge structure (XANES), that Se(VI) was strongly adsorbed to sulfide mineral surfaces by reduction, primarily to Se(IV) on the mineral surface.

Arsenic is commonly assumed to be adsorbed to Fe-oxyhydroxides and remobilized only under moderately to highly reducing conditions (Smedley and Kinniburgh, 2002; Horneman et al., 2004). Typically, As(V) is more strongly adsorbed at neutral pH, although As(III) also shows strong affinity for hydrous Fe-oxide surfaces (Plant et al., 2003). It is possible that As is far-traveled in northern Chile groundwaters because the redox state of groundwaters, like those at the Spence deposit, are close to the Fe^{II}/Fe^{III} transition (Fig. 7), so that Fe^{II}/Fe^{III} ratios are sufficiently elevated to prevent significant retardation of As, without corresponding elevated aqueous Fe concentrations (Horneman et al., 2004). In this case, although Se(IV) is more strongly adsorbed to hydrous Fe-oxides than Se(VI), the occurrence of the Spence groundwaters at the Fe^{II}/Fe^{III} transition would also prevent significant Se(IV) adsorption.

Clearly, based on the filtered and unfiltered aliquots and the fact that Cu concentrations decrease rapidly down-flow of the deposit, unlike the oxyanions, Cu is heavily attenuated. There are significant differences in the filtered and unfiltered samples for Fe and to a lesser extent, Mn. Although Cu might be partially adsorbed to mineral surfaces, if amorphous Fe-oxyhydroxides were significantly fixing Cu, then As and Se should also be immobilized and this appears not to be the case, as discussed above. Thus, loss of Cu from solution may be more closely associated with formation of Cu oxide, chloride and carbonate minerals such as atacamite and

malachite (Fig. 9; see below). Alternatively, copper may be adsorbed to clay surfaces rather than hydrous oxide surfaces. The preferential removal of Cu from Spence groundwaters may also inhibit/prevent the formation of copper-selenides. It is possible that the Se/S ratios are too high for selenides to form and the redox state is still sufficiently oxidizing that sulfides cannot form, thus, Se is mobile. Rhenium behaves differently than Se in post-oxic sediments, displaying no sharp concentration peak suggesting that Re remains fixed in the sediment (Crusius and Thomson, 2003). Rhenium can exist in solution as $Re(OH)_{4(aq)}$ close to the HS^-/SO_4^{2-} boundary over a wide range of pH values (Xiong, 2003b). Xiong (2003b) suggested that the behavior of Re in the Black Sea was more consistent with speciation as $Re(OH)_{4(aq)}$ rather than the commonly assumed ReO_4^-, which is insoluble at higher redox than $Re(OH)_{4(aq)}$.

Reduced forms of Se are not soluble (Kulp and Pratt, 2004). Thus, although the Eh–pH diagram suggests that some Spence waters are stable with respect to Se(0) and selenides (Fig. 7B), the fact that there is essentially no difference in Se concentrations between filtered and unfiltered aliquots (Fig. 6) indicates either that reduced forms of selenium are not present, or that they are adsorbed/coprecipitated with fine colloids that pass through the 0.45 μm filter used in this study. The latter option is considered less likely given the large difference in average filtered versus unfiltered concentrations for the main colloid formers, Fe, Al and Mn (average filtered concentrations are 135, 100 and 240 μg/l for Fe, Al and Mn, respectively, versus average unfiltered concentrations of 6300, 7800 and 1025 μg/l).

Crusius et al. (1996) and Sundby et al. (2004) suggest that both Re and Mo are conservative in seawater and

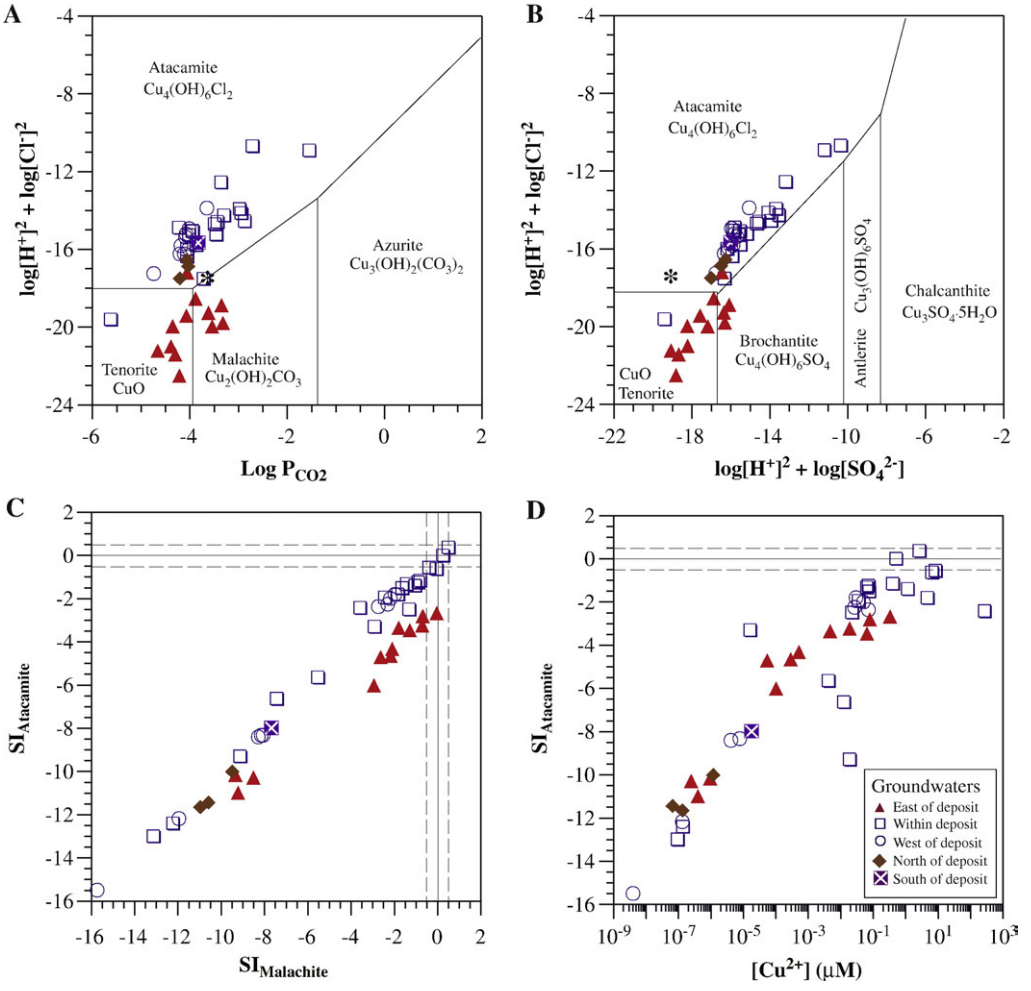

Fig. 9. Activity diagrams showing the relationship between Spence groundwaters and seawater to various copper carbonates, chlorides, sulfates and oxides. Samples with ionic strength >1 are not included.

also in the anoxic portions of the Black Sea water column, and therefore these species are not significantly scavenged onto particulates or precipitated. Robb (2005) suggested that Mo is not reprecipitated following supergene oxidation of Mo-bearing sulfides, but is comprehensively removed via groundwater flow. Seawater has a Re/Mo molar ratio of 0.4 mmol/mol and Crusius et al. (1996) suggested that values well in excess of this ratio indicate suboxic conditions, whereas values close to the seawater ratio would occur under sulfidic conditions. Although other studies of Re, Mo and U in groundwaters and oxic seawater found that near constant ratios indicated conservative behavior for these species (Hodge et al., 1996; Sundby et al., 2004), for the Spence deposit groundwaters variable Re/Mo and U/Re and Mo/Re (Fig. 8) are a function of different sources for U compared to Re and Mo combined with differential speciation in the Spence groundwaters (i.e. non-conservative behavior).

5.5. Implications for supergene and exotic Cu mineralization

There has recently been some debate as to the timing of supergene mineralization in northern Chile, and in particular, the timing of cessation of supergene processes (Alpers and Brimhall, 1988; Sillitoe and McKee, 1996; Hartley and Rice, 2005; Nishiizumi et al., 2005; Arancibia et al., 2006). Some have suggested that hyperarid conditions were attained around 14 Ma, as a consequence of Miocene global climate change related to Andean uplift and propagation of cold upwelling waters along the coast of Chile, consistent with the fact that supergene porphyry mineralization, as dated by K–Ar and Ar–Ar methods, is 14 Ma or older. However, Hartley and Rice (2005) suggest that as more age data becomes available, there is increasing evidence for different periods of cessation of supergene enrichment, at 20, 14 and 6 Ma, and that, based on sedimentological constraints, there was likely also fluctuations in arid/semi-arid conditions between 4 and 3 Ma. Thus, supergene enrichment may have occurred more recently than many models for the climate of northern Chile suggest (Hartley and Rice, 2005).

In addition to supergene copper oxide and sulfide zones, some porphyry systems in northern Chile have associated secondary exotic deposits. Exotic deposits are comprised of copper oxide, silicate, chloride and carbonate minerals, interpreted to have formed as a result of supergene sulfide oxidation, with subsequent transport of Cu via groundwater flow and precipitation some distance from the original sulfide deposit (Münchmeyer, 1996; Mote et al., 2001; Mora et al., 2004). Copper transported away from sulfide mineralization was deposited in paleodrainages in bedrock and gravels. Deposits formed in this manner in northern Chile range in size from small (100–10,000 tonnes; Quebrada Blanca and La Palanada deposits) to large (millions of tonnes; Mina Exotica, El Tesoro) (Münchmeyer, 1996; Mora et al., 2004). Mina Exotica is interpreted to have been derived from the giant Chuquicamata deposit (Alpers and Brimhall, 1988). Exotic copper mineralization in northern Chile is dominated by copper wad, atacamite and paratacamite, and chrysocolla (Mora et al., 2004). During supergene oxidation, acidic Cu^{2+}-bearing waters flow away from hypogene mineralization and the copper is precipitated as the acidic waters are neutralized. Based on our studies at the Spence deposit, we suggest that supergene and exotic processes may be ongoing, rather than having ceased at 9–14 Ma (Alpers and Brimhall, 1988; Arancibia et al., 2006) or 3–6 Ma (Hartley and Rice, 2005).

Groundwaters at the Spence deposit are close to, or exceed, saturation with respect to several secondary Cu minerals such as atacamite, malachite, azurite ($Cu_3(OH)_2(CO_3)_2$), brochantite, antlerite, and chalcanthite. However, the metal concentrations of the recovered groundwaters, combined with the sulfur stable isotopic compositions (Figs. 3, 5), suggest that groundwaters are actively oxidizing sulfides (hypogene and/or supergene) at the Spence deposit. Elevated Cu in the decline water indicates that anthropogenic activity can further enhance sulfide oxidation by increasing exposure to atmospheric oxygen. Secondary copper minerals (e.g., malachite) are abundant within the supergene-enriched zone at the Spence deposit and may have formed primarily prior to 14 Ma. However, mineral saturation calculations (Fig. 9) suggest that secondary copper minerals may be forming under present conditions. Saturation with respect to the copper minerals does not prove that they are actively forming, but is consistent with this interpretation (Cameron et al., 2007).

Recently, Mote et al. (2001) dated copper wad and alunite associated with exotic mineralization at El Salvador. They found that exotic mineralization began around 35 Ma and continued until around 11 Ma, coinciding with supergene oxidation of the El Salvador deposit. Transport of Cu away from porphyry mineralization and formation of exotic mineralization ceased in the Middle Miocene owing to enhanced dessication of the Atacama Desert (Mote et al., 2001). Although the bulk of exotic mineralization apparently stopped in mid-Miocene times, the results from the Spence deposit indicate that the current groundwater regime may be

capable of producing limited amounts of exotic copper mineralization that are deposited within or close to the deposit. Present groundwaters at Spence are not sufficiently acid-producing to mobilize large amounts of copper and transport it away from the deposit.

6. Conclusions

Groundwaters at the Spence porphyry copper deposit, Atacama Desert, northern Chile are characterized by elevated concentrations of metals and metalloids characteristic of this style of ore deposit. Groundwaters upflow of the deposit represent the regional groundwaters and are characterized by relatively low concentrations of metals and metalloids characteristics of porphyry copper ores in northern Chile, i.e., Cu, Mo, Se, Re, As. In contrast, most ore-related metals, metalloids and SO_4 are elevated (Se up to 800 μg/l, Re up to 31 μg/l, Mo up to 475 μg/l and As up to 300 μg/l) in groundwaters within and down-flow of the deposit. Similarly, copper (up to 1300 μg/l; decline water=29,000 mg/l) and some other metal cations (e.g., Pb, Zn, Ni, and Co) have elevated concentrations in groundwaters within the deposit, but lower concentrations down-flow of the deposit. Within the deposit, regional meteoric waters from the east mix with saline waters of deep origin. Elevated salinities down-flow from the deposit indicates that inflow of saline waters dominates. The concentrations of ore-associated metals and metalloids are elevated in these groundwaters after accounting for changes in salinity indicating that these groundwaters have interacted with the porphyry copper ore. Coincident with increasing concentrations of ore-associated metals and metalloids, groundwaters $\delta^{34}S_{CTD}$ ratios decrease from regional values (+5 to +8‰) towards ore-values (around 0‰), consistent with groundwater–deposit interaction.

The different behavior of Se, Re, As and Mo compared to Cu in the Spence groundwaters is probably a function of speciation of the metals and metalloids and Eh–pH conditions of the groundwaters; the former group behave as anions or neutral species in these groundwaters, enhancing their mobility, whereas the base metals are present as cations and are lost from solution most likely through adsorption to colloidal material, consistent with differences in filtered/unfiltered ratios.

Our groundwater geochemical data from the Spence deposit indicate that sulfides (in the hypogene and/or supergene zones) are being oxidized under the present conditions and mineral saturation calculations suggest that secondary copper minerals (antlerite, atacamite, malachite) may also be actively forming. Thus, supergene mineralization processes may be ongoing, despite the hyperarid conditions and the assumption that these processes ceased in the mid-Miocene or towards the end of the Miocene.

Acknowledgements

Alexi Ramirez (RioChilex) is thanked for his assistance with much of the groundwater sampling. Daniel Salinas (Rio Tinto) is especially thanked for assistance in soil and groundwater sampling. We thank Dan Layton-Matthews for discussion regarding the chemistry of Se. Gwendy Hall, Judy Vaive, and Peter Belanger at the Geological Survey of Canada are thanked for the 1999 geochemical results, the Geochemistry Laboratory in the Geosciences Department at UTD for the 2000 data. Wendy Abdi (University of Ottawa) and Steve Taylor (University of Calgary) are thanked for overseeing the stable isotope analyses. Karen Johannesson is thanked for insightful comments on an earlier version of the manuscript. The paper benefited greatly from thorough and insightful reviews by two anonymous journal reviewers and Editor David Rickard.

References

Alpers, C.N., Brimhall, G.H., 1988. Middle Miocene climatic change in the Atacama Desert, northern Chile: evidence from supergene mineralization at La Escondida. Geological Society of America Bulletin 100, 1640–1656.

Anbar, A.D., Creaser, R.A., Papanastassiou, D.A., Wasserburg, G.J., 1992. Rhenium in seawater: confirmation of generally conservative behavior. Geochimica et Cosmochimica Acta 56, 4099–4103.

Arancibia, G., Matthews, S.J., De Arce, C.P., 2006. K–Ar and Ar-40/Ar-39 geochronology of supergene processes in the Atacama Desert, Northern Chile: tectonic and climatic relations. Journal of the Geological Society 163, 107–118.

Audétat, A., Pettke, T., 2006. Evolution of a porphyry–Cu mineralized magma system at Santa Rita, New Mexico (USA). Journal of Petrology 47, 2021–2046.

Balistrieri, L.S., Chao, T.T., 1990. Adsorption of selenium by amorphous iron oxyhydroxide and manganese dioxide. Geochimica et Cosmochimica Acta 54, 739–751.

Ball, J.W., Nordstrom, D.K., 1991. Users manual for WATEQ4F with revised thermodynamic database and test cases for calculating speciation of major, trace, and redox elements in natural waters. USGS Open-File Report 91–183.

Bates, R.G., Culberson, C.H., 1977. Hydrogen ions and the thermodynamic state of marine systems. In: Anderson, N.R., Malahoff, A. (Eds.), The Fate of Fossil Fuel CO_2 in the Oceans. Plenum Press, New York, N.Y., United States (USA), pp. 45–61.

Bethke, C.M., 1994. The Geochemist's Workbench. University of Illinois.

BHP-Billiton, L., 2007. http://www.bhpbilliton.com.au/bbContentRepository/spenceanalystvisit19march2007.pdf./url>.

Boult, K.A., Cowper, M.M., Heath, T.G., Sato, H., Shibutani, T., Yui, M., 1998. Towards an understanding of the sorption of U(VI) and Se(IV) on sodium bentonite. Journal of Contaminant Hydrology 35, 141–150.

Boyle, D.R., 2003. Preglacial weathering of massive sulfide deposits in the Bathurst Mining Camp: economic geology, geochemistry, and exploration applications. In: Goodfellow, W.D., McCutcheon, S.R., Peter, J.M. (Eds.), Massive Sulphide Deposits of the Bathurst Mining Camp. New Brunswick, and Northern Maine, pp. 689–721.

Brookins, D.G., 1988. Eh–pH Diagrams for Geochemistry. Springer-Verlag. 176 pp.

Caceres, D.D., Pino, P., Montesinos, N., Atalah, E., Amigo, H., Loomis, D., 2005. Exposure to inorganic arsenic in drinking water and total urinary arsenic concentration in a Chilean population. Environmental Research 98, 151–159.

Cameron, E.M., Hamilton, S.M., Leybourne, M.I., Hall, G.E.M., McClenaghan, B., 2004. Finding deeply-buried deposits using geochemistry. Geochemistry: Exploration, Environment, Analysis 4, 7–32.

Cameron, E.M., Leybourne, M., Venegas, R.C., Vásquez, A.R., 2000. Preliminary Report: Geochemical Data for Soils over the Gaby Sur deposit. Chile, CAMIRO Deep-Penetrating Geochemistry, Phase II. 13 pp.

Cameron, E.M., Leybourne, M.I., Palacios, C., 2007. Atacamite in the oxide zone of copper deposits in northern Chile: involvement of deep formation waters? Mineralium Deposita 42, 205–218.

Carmona, V., Pueyo, J.J., Taberner, C., Chong, G., Thirlwall, M., 2000. Solute inputs in the Salar de Atacama (N. Chile). Journal of Geochemical Exploration 69–70, 449–452.

Chávez, W.X., 2000. Supergene oxidation of copper deposits: zoning and distribution of copper oxide minerals. Society of Economic Geologists Newsletter 41, 1–21.

Cheatham, M.M., Sangrey, W.F., White, W.M., 1993. Sources of error in internal calibration ICP-MS analysis of geological samples and an improved non-linear drift correction procedure. Spectrochimica Acta 48B, E487–E506.

Christian, W.J., Hopenhayn, C., Centeno, J.A., Todorov, T., 2006. Distribution of urinary selenium and arsenic among pregnant women exposed to arsenic in drinking water. Environmental Research 100, 115–122.

Clark, I.D., Raven, K.G., 2004. Sources and circulation of water and arsenic in the giant mine, Yellowknife, NWT, Canada. Isotopes in Environment and Health Studies 40, 1–14.

Crusius, J., Calvert, S., Pedersen, T., Sage, D., 1996. Rhenium and molybdenum enrichments in sediments as indicators of oxic, suboxic and sulfidic conditions of deposition. Earth and Planetary Science Letters 145, 65–78.

Crusius, J., Thomson, J., 2003. Mobility of authigenic rhenium, silver, and selenium during postdepositional oxidation in marine sediments. Geochimica et Cosmochimica Acta 67, 265–273.

Cuadra, C.C., Rojas, G.S., 2001. Oxide mineralization at the Radomiro Tomic porphyry copper deposit, northern Chile. Economic Geology 96, 387–400.

Dalai, T.K., Singh, S.K., Trivedi, J.R., Krishnaswami, S., 2002. Dissolved rhenium in the Yamuna River system and the Ganga in the Himalaya: role of black shale weathering on the budgets of Re, Os, and U in rivers and CO_2 in the atmosphere. Geochimica et Cosmochimica Acta 66, 29–44.

Deverel, S., Fio, J., Dubrovsky, N., 1994. Distribution and mobility of selenium in groundwater in agricultural areas, Western San Josquin Valley, California. In: Frankenberger, W.T., Benson, S. (Eds.), Selenium in the Environment. Dekker, New York, pp. 157–183.

Dold, B., Spangenberg, J.E., 2002. Study of water-soluble sulfates in tailings profiles from porphyry copper deposits by sulfur and oxygen isotopes, 12th Annual Goldschmidt Conference. 12th Annual Goldschmidt Conference. Davos, Switzerland, August 18–23. Geochimica et Cosmochmica Acta, vol. 66, supplement 1, p. 189.

Engberg, R.A., 1999. Selenium budgets for Lake Powell and the upper Colorado River Basin. Journal of the American Water Resources Association 35, 771–786.

Field, C.W., Gustafson, L.B., 1976. Sulfur isotopes in the porphyry copper deposit at El Salvador. Economic Geology 71, 1533–1548.

Freydier, C., Ruiz, J., Chesley, J., McCandless, T., Munizaga, F., 1997. Re–Os isotope systematics of sulfides from felsic igneous rocks: application to base metal porphyry mineralization in Chile. Geology 25, 775–778.

Gieskes, J.M., Gamo, T., Brumsack, H., 1991. Chemical methods for interstitial water analysis aboard Joides Resolution. Ocean Drilling Program, Technical Note 15, 60.

Hartley, A.J., Rice, C.M., 2005. Controls on supergene enrichment of porphyry copper deposits in the central Andes: a review and discussion. Mineralium Deposita 40, 515–525.

Hodge, V.F., Johannesson, K.H., Stetzenbach, K.J., 1996. Rhenium, molybdenum, and uranium in groundwater from the southern Great Basin, USA: evidence for conservative behaviour. Geochimica et Cosmochimica Acta 60, 3197–3214.

Horneman, A., van Geen, A., Kent, D.V., Mathe, P.E., Zheng, Y., Dhar, R.K., O'Connell, S., Hoque, M.A., Aziz, A., Shamsdduha, M., Seddique, A.A., Ahmed, K.M., 2004. Decoupling of As and Fe release to Bangladesh groundwater under reducing conditions. Part I: evidence from sediment profiles. Geochimica et Cosmochimica Acta 68, 3459–3473.

Howard, J.H., 1977. Geochemistry of selenium: formation of ferrosilite and selenium behavior in the vicinity of oxidizing sulfide and uranium deposits. Geochimica et Cosmochimica Acta 41, 1665–1678.

Jaffe, L.A., Peucker-Ehrenbrink, B., Petsch, S.T., 2002. Mobility of rhenium, platinum group elements and organic carbon during black shale weathering. Earth and Planetary Science Letters 198, 339–353.

Johannesson, K.H., Stetzenbach, K.J., Kreamer, D.K., Hodge, V.F., 1996. Multivariate statistical analysis of arsenic and selenium concentrations in groundwaters from south-central Nevada and Death Valley, California. Journal of Hydrology 178, 181–204.

Kent, D.B., Davis, J.A., Anderson, L.C.D., Rea, B.A., 1995. Transport of chromium and selenium in a pristine sand and gravel aquifer; role of adsorption processes. Water Resources Research 31, 1041–1050.

Kent, D.B., Davis, J.A., Anderson, L.C.D., Rea, B.A., Waite, T.D., 1994. Transport of chromium and selenium in the suboxic zone of a shallow aquifer; influence of redox and adsorption reactions. Water Resources Research 30, 1099–1114.

Kulp, T.R., Pratt, L.M., 2004. Speciation and weathering of selenium in Upper Cretaceous chalk and shale from South Dakota and Wyoming, USA. Geochimica et Cosmochimica Acta 68, 3687–3701.

Langmuir, D., 1997. Aqueous Environmental Geochemistry. Prentice-Hall, Upper Saddle River, NJ. 600 pp.

Layton-Matthews, D., Peter, J.M., Scott, S.D. and Leybourne, M.I., in press. Distribution, mineralogy, and geochemistry of Selenium in felsic volcanic-hosted Massive Sulfide Deposits of the Finlayson Lake Area, Yukon Territory, Canada: implications for source, transport, and depositional controls. Economic Geology.

Leybourne, M.I., 2007. Aqueous geochemistry in mineral exploration. In: Goodfellow, W.D. (Ed.), Mineral Resources of Canada: A Synthesis of Major Deposit-types, District Metallogeny, the Evolution of Geological Provinces, and Exploration Methods, pp. 1007–1034.

Leybourne, M.I., Cameron, E.M., 2006. Composition of groundwaters associated with porphyry–Cu deposits, Atacama Desert, Chile:

elemental and isotopic constraints on water sources and water–rock reactions. Geochimica et Cosmochimica Acta 70, 1616–1635.

Leybourne, M.I., Goodfellow, W.D., 2003. Processes of metal solution and transport in ground waters interacting with undisturbed massive sulfide deposits, Bathurst Mining Camp, New Brunswick. In: Goodfellow, W.D., McCutcheon, S.R., Peter, J.M. (Eds.), Massive Sulphide Deposits of the Bathurst Mining Camp. New Brunswick, and Northern Maine, pp. 723–740.

Leybourne, M.I., Goodfellow, W.D., Boyle, D.R., 1998. Hydrogeochemical, isotopic, and rare earth element evidence for contrasting water–rock interactions at two undisturbed Zn–Pb massive sulphide deposits, Bathurst Mining Camp, N.B., Canada. Journal of Geochemical Exploration 64, 237–261.

Mathur, R., Ruiz, J., Munizaga, F., 2000. Relationship between copper tonnage of Chilean base-metal porphyry deposits and Os isotope ratios. Geology 28, 555–558.

McCandless, T.E., Ruiz, J., Campbell, A.R., 1993. Rhenium behavior in molybdenite in hypogene and near-surface environments: implications for Re–Os geochronology. Geochimica et Cosmochimica Acta 57, 889–905.

Mora, R., Artal, J., Brockway, H., Martinez, E., Muhr, R., 2004. El Tesoro exotic copper deposit, Antofagasta region, northern Chile. Special Publication (Society of Economic Geologists (U S) 11, 187–197.

Morris, D.F., 1969. Rhenium. In: Wedepohl, K.H. (Ed.), Handbook of Geochemistry, II-5. Springer, Berlin, Germany, pp. 75–A-1–75-A-2.

Mote, T.I., Becker, T.A., Renne, P., Brimhall, G.H., 2001. Chronology of exotic mineralization at El Salvador, Chile, by $^{40}Ar/^{39}Ar$ dating of copper wad and supergene alunite. Economic Geology 96, 351–366.

Münchmeyer, C., 1996. Exotic deposits — products of lateral migration of supergene solutions from porphyry copper deposits. In: Camus, F., Sillitoe, R.H., Petersen, R. (Eds.), Andean copper deposits: new discoveries, mineralization, styles and metallogeny. Society of Economic Geologists, pp. 43–58.

Myneni, S.C.B., Tokunaga, T.K., Brown, G.E., 1997. Abiotic selenium redox transformations in the presence of Fe(II,III) oxides. Science 278, 1106–1109.

Nishiizumi, K., Caffee, M.W., Finkel, R.C., Brimhall, G., Mote, T., 2005. Remnants of a fossil alluvial fan landscape of Miocene age in the Atacama Desert of northern Chile using cosmogenic nuclide exposure age dating. Earth and Planetary Science Letters 237, 499–507.

Ossandon, G., Freraut, R., Gustafson, L.B., Lindsay, D.D., Zentilli, M., 2001. Geology of the Chuquicamata mine: a progress report. Economic Geology 96, 249–270.

Oyarzun, R., Guevara, S., Oyarzun, J., Lillo, J., Maturana, H., Higueras, P., 2006. The As-contaminated Elqui river basin: a long lasting perspective (1975–1995) covering the initiation and development of Au–Cu–As mining in the high Andes of northern Chile. Environmental Geochemistry and Health 28, 431–443.

Palacios, C., Ramírez, L.E., Townley, B., Solari, M., Guerra, N., 2007. The role of the Antofagasta — Calama Lineament in ore deposit formation in the Andes of northern Chile. Mineralium Deposita 41.

Parkhurst, D.L., Appelo, C.A.J., 1999. User's guide to PHREEQC (version 2); a computer program for speciation, batch-reaction, one-dimensional transport, and inverse geochemical calculations. Water-Resources Investigations — U. S. Geological Survey, Report WRI 99–4259 312 pp.

Peters, G.M., Maher, W.A., Jolley, D., Carroll, B.I., Gomes, V.G., Jenkinson, A.V., McOrist, G.D., 1999. Selenium contamination, redistribution and remobilization in sediments of Lake Macquarie, NSW. Organic Geochemistry 30, 1287–1300.

Phipps, G.C., Boyle, D.R., Clark, I.D., 2004. Groundwater geochemistry and exploration methods: Myra Falls volcanogenic massive-sulphide deposits, Vancouver Island, British Columbia, Canada. Geochemistry: Exploration, Environment, Analysis 4, 329–340.

Plant, J.A., Kinniburgh, D.G., Smedley, P.L., Fordyce, F.M., Klinck, B. A., 2003. Arsenic and Selenium, Treatise on Geochemistry. Elsevier 17–66.

Pueyo, J.J., Chong, G., Jensen, A., 2001. Neogene evaporites in desert volcanic environments: Atacama Desert, northern Chile. Sedimentology 48, 1411–1431.

Rasmussen, P.E., Friske, P.W.B., Azzaria, L.M., Garrett, R.G., 1998. Mercury in the Canadian environment, current research challenges. Geoscience Canada 25, 1–13.

Rech, J.A., Quade, J., Hart, W.S., 2003. Isotopic evidence for the source of Ca and S in soil gypsum, anhydrite and calcite in the Atacama Desert, Chile. Geochimica et Cosmochimica Acta 67, 575–586.

Richards, J.P., Noble, S.R., Pringle, M.S., 1999. A revised Late Eocene age for porphyry magmatism in the Escondida area, northern Chile. Economic Geology 94, 1231–1248.

Robb, L.J., 2005. Introduction to Ore-forming Processes. Blackwell. 373 pp.

Romero, L., Alonso, H., Campano, P., Fanfani, L., Cidu, R., Dadea, C., Keegan, T., Thornton, I., Farago, M., 2003. Arsenic enrichment in waters and sediments of the Rio Loa (Second Region, Chile). Applied Geochemistry 18, 1399–1416.

Rowland, M.D., Clark, A.H., 2001. Temporal overlap of supergene alteration and high-sulphidation mineralization in the Spence porphyry copper deposit, II Region, Chile. Geological Society of America Annual Meeting 2001.

Runnells, D.D., Lindberg, R.D., 1990. Selenium in aqueous solutions: the impossibility of obtaining meaningful Eh using a platinum electrode, with implications for modeling of natural waters. Geology 18, 212–215.

Selinus, O., Alloway, B., Centeno, J.A., Finkelman, R.B., Fuge, R., Lindh, U., Smedley, P. (Eds.), 2005. Essentials of Medical Geology: Impacts of the Natural Environment on Public Health. Elsevier Academic Press. 812 pp.

Sillitoe, R., McKee, E., 1996. Age of supergene oxidation and enrichment in the Chilean Porphyry Copper Province. Economic Geology 91, 164–179.

Sillitoe, R.H., 1992. Gold and copper metallogeny of the central Andes — past, present, and future exploration objectives. Economic Geology 87, 2205–2216.

Sillitoe, R.H., 2000. Gold-rich porphyry deposits: descriptive and genetic models and their role in exploration and discovery. Reviews in Economic Geology 13, 315–344.

Simon, G., Essene, E.J., 1996. Phase relations among selenides, sulfides, tellurides, and oxides: I. thermodynamic properties and calculated equilibria. Economic Geology 91, 1183–1208.

Simon, G., Kesler, S.E., Essene, E.J., 1997. Phase relations among selenides, sulfides, tellurides, and oxides: II. applications to selenide-bearing ore deposits. Economic Geology 92, 468–484.

Smedley, P.L., Kinniburgh, D.G., 2002. A review of the source, behaviour and distribution of arsenic in natural waters. Applied Geochemistry 17, 517–568.

Sohrin, Y., Matsui, M., Nakayama, E., 1999. Contrasting behavior of tungsten and molybdenum in the Okinawa Trough, the East China Sea and the Yellow Sea. Geochimica Et Cosmochimica Acta 63, 3457–3466.

Sundby, B., Martinez, P., Gobiel, C., 2004. Comparitive geochemistry of cadmium, rhenium, uranium, and molybdenum in continental margin sediments. Geochimica et Cosmochimica Acta 68, 2485–2493.

Tachi, Y., Shibutani, T., Sato, H., Yui, M., 1998. Sorption and diffusion behavior of selenium in tuff. Journal of Contaminant Hydrology 35, 77–89.

Thoral, S., Rose, J., Van Geen, L., Garnier, J.M., Chapon, V., Hazeman, J.L., Heulin, T., Bottero, J.Y., 2005. Oxidation of natural groundwater from Bangladesh: arsenic speciation evolution assessed by XAS. Geochimica Et Cosmochimica Acta 69, A615–A615.

Thornber, M.R., 1975. Supergene alteration of sulphides, I. A chemical model based on massive nickel sulphide deposits at Kambalda, Western Australia. Chemical Geology 15, 1–14.

Tosdal, R.M., Richards, J.P., 2001. Magmatic and structural controls on the development of Cu±Mo±Au deposits. Reviews in Economic Geology 14, 157–181.

Van Geen, A., Rose, J., Thoral, S., Garnier, J.M., Zheng, Y., Bottero, J.Y., 2004. Decoupling of As and Fe release to Bangladesh groundwater under reducing conditions. Part II: evidence from sediment incubations. Geochimica Et Cosmochimica Acta 68, 3475–3486.

Xiong, Y., 2003a. Predicted equilibrium constants for solid and aqueous selenium species to 300 °C: applications to selenium-rich mineral deposits. Ore Geology Reviews 23, 259–276.

Xiong, Y., 2003b. Solubility and speciation of rhenium in anoxic environments at ambient temperature and applications to the Black Sea. Deep-Sea Research I 50, 681–690.

Xiong, Y., Wood, S.A., 1999. Experimental determination of the solubilty of ReO_2 and the dominant oxidation state of rhenium in hydrothermal solutions. Chemical Geology 158, 245–256.

Yllera de Llano, A., Bidoglio, G., Avogadro, A., Gibson, P.N., Rivas Romero, P., 1996. Redox reactions and transport of selenium through fractured granite. Journal of Contaminant Hydrology 21, 129–139.